

1 Subunit-selective proteasome activity profiling uncovers uncoupled 2 proteasome subunit activities during bacterial infections

3
4 Johana C. Misas-Villamil^{1,2}, Aranka M. van der Burgh^{1,8}, Friederike Grosse-Holz⁷, Marcel Bach-
5 Pages⁷, Judit Kovács^{1,6}, Farnusch Kaschani³, Sören Schilasky¹, Asif Emron Khan Emon^{1,4}, Mark
6 Ruben⁵, Markus Kaiser³, Hermen S. Overkleeft⁵, and Renier A. L. van der Hoorn^{1,7*}

7
8 ¹ The Plant Chemetics Laboratory, Max Planck Institute for Plant Breeding Research, Carl-von-Linné
9 Weg 10, 50829 Cologne, Germany

10 ² Botanical Institute and Cluster of Excellence on Plant Sciences, University of Cologne, 50674
11 Cologne, Germany

12 ³ Chemical Biology, Universität Duisburg-Essen, Zentrum für Medizinische Biotechnologie, Fakultät
13 für Biologie, Universitätsstr. 2, 45117 Essen, Germany

14 ⁴ Current address: Bonn-Aachen International Center for IT, University of Bonn, Dahlmannstrasse 2,
15 53113 Bonn, Germany

16 ⁵ Institute of Chemistry and Netherlands Proteomics Centre, Gorlaeus Laboratories, 2333 CC Leiden,
17 The Netherlands

18 ⁶ Department of Plant Biology, University of Szeged, Szeged, Hungary

19 ⁷ The Plant Chemetics Laboratory, Department of Plant Sciences, University of Oxford, South Parks
20 Lane OX1 3RB Oxford, United Kingdom

21 ⁸ Current address: Laboratory for Phytopathology, Wageningen University, Droevendaalsesteeg 1,
22 6708 PB Wageningen, The Netherlands.

23
24 *, for correspondence: renier.vanderhoorn@plants.ox.ac.uk

25
26 **Keywords:** catalytic subunit; core protease; *Arabidopsis thaliana*; *Nicotiana benthamiana*; Activity-
27 based protein profiling; proteasome manipulation.

28
29 **Running head:** Subunit-selective proteasome activity profiling

30
31 **Significances Statement:** Proteasome activity profiling with subunit-selective fluorescent probes is a
32 robust way to display activities of $\beta 1$ and $\beta 5$ activities in any plant species. We validate these next
33 generation tools and use it to uncover that $\beta 1$ and $\beta 5$ activities are uncoupled upon infection by
34 virulent bacteria.

35
36 **SUMMARY**

37 **The proteasome is a nuclear - cytoplasmic proteolytic complex involved in nearly all regulatory**
38 **pathways in plant cells. The three different catalytic activities of the proteasome can have**
39 **different functions but tools to monitor and control these subunits selectively are not yet**
40 **available in plant science. Here, we introduce subunit-selective inhibitors and dual-color**
41 **fluorescent activity-based probes for studying two of the three active catalytic subunits of the**
42 **plant proteasome. We validate these tools in two model plants and use this to study the**
43 **proteasome during plant-microbe interactions. Our data reveals that *Nicotiana benthamiana***
44 **incorporates two different paralogs of each catalytic subunit into active proteasomes.**
45 **Interestingly, both $\beta 1$ and $\beta 5$ activities are significantly increased upon infection with pathogenic**
46 ***Pseudomonas syringae* pv. *tomato* DC3000 lacking hopQ1-1 (PtoDC3000(Δ hQ)) whilst the**
47 **activity profile of the $\beta 1$ subunit changes. Infection with wild-type PtoDC3000 causes**
48 **proteasome activities that range from strongly induced $\beta 1$ and $\beta 5$ activities to strongly**
49 **suppressed $\beta 5$ activities, revealing that $\beta 1$ and $\beta 5$ activities can be uncoupled during bacterial**
50 **infection. These selective probes and inhibitors are now available to the plant science community**
51 **and can be widely and easily applied to study the activity and role of the different catalytic**
52 **subunits of the proteasome in different plant species.**

53

54 **INTRODUCTION**

55 The ubiquitin proteasome pathway is responsible for the selective degradation of proteins in the cell
56 regulating numerous cellular and physiological functions. The proteasome is a multi-subunit, ATP-
57 dependent proteolytic complex consisting of a 20S core particle (CP) and a 19S regulatory particle
58 (RP) (Groll et al., 1997). The CP is ubiquitin and ATP independent, and consists of four stacked rings
59 forming a barrel. The inner two rings of the barrel consist of β subunits and these are flanked by two
60 rings of α subunits (Kurepa and Smalle, 2008a). Each ring consists of seven subunits. The catalytic
61 subunits responsible for peptide cleavage are located in the β rings and have an active site N-terminal
62 Threonine (Thr). The catalytic β subunits have different proteolytic activities: $\beta 1$ has caspase-like
63 activity, $\beta 2$ trypsin-like activity and $\beta 5$ chymotrypsin-like activity (Dick et al., 1998).

64 In addition to its crucial role in plant hormone signaling, the ubiquitin proteasome pathway
65 has received attention in the plant pathogen field because several pathogens target this system. The
66 proteasome acts as a hub in various immune signalling cascades, and is therefore an obvious target for
67 pathogens (Üstün et al., 2016). Pathogen-derived effectors were found to interact with components of
68 the ubiquitin proteasome system such as E3-ligases, F-box proteins and SUMO de-conjugation
69 enzymes (Banfield et al., 2015). These effectors interfere in vesicle trafficking or promote
70 transcription factor degradation. Some of these bacterial effectors act by inhibiting the proteasome.
71 For instance, the XopJ effector produced by *Xanthomonas campestris* pv. *vesicatoria* and the HopZ4
72 effector from *Pseudomonas syringae* pv. *lachrymans* interact with the RPT6 subunit of the 19S
73 regulatory particle, suppressing the activity of the proteasome and repressing salicylic acid (SA)

74 mediated responses (Üstün et al., 2013; 2014). In addition, the non-ribosomal polypeptide Syringolin
75 A (SylA) secreted by *Pseudomonas syringae* pv. *syringae* also targets the proteasome (Groll et al.,
76 2008), in this case by covalently inhibiting $\beta 2$ and $\beta 5$ subunits of the plant proteasome (Kolodziejek et
77 al. 2011). SylA facilitates opening of stomata and promotes bacterial colonization from wound sites
78 (Misas-Villamil et al., 2013; Schellenberg et al., 2010).

79 So far, the plant proteasome could not be sufficiently investigated due to technical limitations
80 and lack of suitable approaches. First, reverse genetic approaches are challenging since mutations in
81 CP subunits usually cause severe pleiotropic defects or even lethality (Kurepa and Smalle, 2008a).
82 Roles of the different CP subunits are also impossible to study using a knockout approach since the CP
83 requires integrity for its function. Second, a number of proteasome subunits are modified post-
84 translationally, e.g. by proteolytic processing, acetylation and ubiquitylation (Book et al., 2010). Third,
85 the proteasome is a versatile complex in which substrate specificities can be changed, depending on
86 the assembly of the different subunits. The most notable example is the immunoproteasome in
87 mammals in which constitutive subunits of the CP are replaced by inducible subunits (Aki et al.,
88 1994). The recently discovered replacement of $\alpha 3$ by $\alpha 4$ in human proteasomes is another example of
89 alternative proteasomes (Padmanabhan et al., 2016). Although there is no evidence that plants have an
90 alternative proteasome, plant genomes carry multiple genes for nearly each subunit (Yang et al., 2004)
91 and the proteasome in *Arabidopsis* is assembled with paralogous pairs for most subunits (Book et al.,
92 2010). Remarkably, tobacco genes encoding $\beta 1$, $\alpha 3$ and $\alpha 6$ subunits are transcriptionally upregulated
93 after treatment with the elicitor cryptogein (Suty et al., 2003) indicating that plants might assemble
94 inducible alternative proteasomes.

95 The activity of the proteasome subunits can be studied using fluorogenic substrates, which
96 require the isolation and purification of the proteasome, a very tedious and laborious method only
97 applicable on certain soft plant tissues (Yang et al., 2004; Book et al., 2010). We previously
98 introduced activity-based protein profiling (ABPP) to monitor the activity of the plant proteasome (Gu
99 et al., 2010). ABPP relies on the use of small molecule chemical probes that are composed of a
100 reactive group, a linker and a reporter tag that can be biotin or fluorescent to facilitate protein
101 purification and detection, respectively (Cravatt et al., 2008). These chemical probes react with the
102 active site of enzymes, resulting in a covalent and often irreversible labeling, which facilitates the
103 detection, purification and identification of those labeled proteins. Labeling reflects protein activity
104 rather than abundance because the probes only react when the active site is available and reactive and
105 many enzymes are regulated by changes in the availability and reactivity of the active site. So far we
106 have introduced over 40 activity-based probes into plant science to monitor e.g. Cys proteases,
107 glycosidases, subtilases, acyltransferases and glutathione transferases, and many of these probes are
108 widely used in plant science (Morimoto and Van der Hoorn, 2016). DCG-04, for instance, is a probe
109 for papain-like Cys proteases (Greenbaum et al., 2000; Van der Hoorn et al., 2004) that has been
110 instrumental for the discovery of pathogen-derived inhibitors (Rooney et al., 2005; Tian et al., 2007;

111 Shabab et al., 2008; Van Esse et al., 2008; Song et al., 2009; Kaschani et al., 2010; Lozano-Torres et
112 al., 2012; Mueller et al., 2013), deciphering protease-inhibitor arms-races and effector adaptation upon
113 a host jump (Hörger et al., 2012; Dong et al., 2014), and identifying senescence-associated proteases
114 (Martinez et al., 2007; Carrion et al., 2013; Porret et al., 2015). Likewise, proteasome probes have
115 been used to describe post-translational activation of the proteasome during salicylic acid signaling
116 (Gu et al., 2010), the selective suppression of the nuclear proteasome by bacterial phytotoxin
117 Syringolin A (SylA, Kolodziejek et al., 2011; Misas-Villamil et al., 2013); and the regulation of the
118 proteasome by NAC transcription factor RPX (Nguyen et al., 2013), the validation and availability of
119 next generation chemical probes will underpin exciting scientific discoveries.

120 The activity of the three catalytic subunits of the Arabidopsis proteasome can be easily
121 distinguished using ABPP since these subunits have different molecular weight (MW) (Gu et al.,
122 2010; Kolodziejek et al., 2011). In other plants, however, the MW of these different subunits can
123 overlap and multiple subunit genes can cause additional signals that are difficult to annotate (Gu,
124 2010). In the model plant *Nicotiana benthamiana*, for instance, all three different catalytic subunits
125 were detected in a single band (Misas-Villamil et al., 2013). Here, we describe subunit-specific
126 labeling for two catalytic subunits. By using these next generation probes we are able to display
127 activities of $\beta 1$ and $\beta 5$ catalytic subunits in *N. benthamiana*, revealing that activity of these subunits
128 independently change upon bacterial infection.

129

130 RESULTS

131 *LW124 and MVB127 are selective probes for the $\beta 1$ and $\beta 5$ catalytic subunits*

132 We have previously used MVB072 (**Figure 1a**), a probe that labels all three catalytic subunits of the
133 plant proteasome (Kolodziejek et al., 2011). Labeling of Arabidopsis leaf extracts with MVB072
134 results in three signals representing $\beta 2$ (top band 1), $\beta 5$ (middle band 2) and $\beta 1$ (bottom band 3)
135 (**Figure 1b**, Kolodziejek et al., 2011). We also have previously introduced a rhodamine-tagged SylA
136 (RhSylA, **Figure 1a**) which preferentially labels $\beta 2$ (top band 6), and $\beta 5$ (bottom band 7) (**Figure 1b**,
137 Kolodziejek et al., 2011).

138 Here we introduce two next generation probes for labeling of specific proteasome catalytic
139 subunits. LW124 contains an epoxyketone reactive group, the tetrapeptide Ala-Pro-Nle-Leu and a
140 bodipy Cy2 fluorescent group (**Figure 1a**, Li et al., 2013). MVB127 has a vinyl sulphone (VS)
141 reactive group, a MeTyr-Phe-Ile tripeptide and a bodipy Cy2 fluorescent group with an azide group
142 that can be used for click chemistry reactions (**Figure 1a**, Li et al., 2013). In contrast to MVB072
143 labeling, which in Arabidopsis results in three signals, we detect only one signal for LW124 at 26 kDa
144 (**Figure 1b**, band 4), and one signal for MVB127 at ca. 27 kDa (**Figure 1b**, band 5). No strong signals
145 appear in the remainder of the gels (Supplemental **Figure S1**). All signals are caused by proteasome
146 labeling since they are suppressed upon pre-incubation with the selective proteasome inhibitor
147 epoxomicin (Supplemental **Figure S2**).

148 Because LW124 carries a different fluorophore, we tested if these probes can be mixed and
149 used in co-labeling experiments. Co-labeling by adding two probes at the same time and with the same
150 concentration to Arabidopsis leaf extracts indeed shows specific signals for both probes (**Figure 1c**).
151 The bottom signal (band 3, β 1) of MVB072 is suppressed upon co-labeling with LW124 (**Figure 1c**,
152 lane 4), indicating that LW124 targets β 1 of the Arabidopsis proteasome. The overlay shows that the
153 β 1-LW124 conjugate (band 4) migrates slightly faster in the protein gel than the β 1-MVB072
154 conjugate (band 3), consistent with the different MW of the two probes (**Figure 1b** and **1c**, lanes 1 and
155 2). A suppression of labeling cannot be observed upon co-labeling of MVB072 with MVB127 since
156 they carry the same fluorophore (**Figure 1c**, lane 5). Co-labeling of LW124 with MVB127 results in
157 two signals (**Figure 1c**, top two panels, lane 6), indicating that these probes label different subunits.
158 However, the MVB127 signal (band 5) is suppressed upon colabeling with LW124 (**Figure 1c**, lanes 3
159 and 6). By contrast, labeling by LW124 (band 4) seems unaffected upon co-labeling with MVB127
160 (**Figure 1c**, lanes 2 and 6).

161 To confirm that LW124 and MVB127 are specific probes for one proteasome catalytic
162 subunit, we pre-incubated the samples with subunit-specific proteasome inhibitors that have been
163 validated on mammalian proteasomes. N3 β 1 is an epoxyketone inhibitor that targets the β 1 catalytic
164 subunit, whereas N3 β 5 is a vinyl sulphone inhibitor of the β 5 catalytic subunit (**Figure 2a**, Verdoes et
165 al., 2010). Notably, these are non-fluorescent versions of the probes since the peptide and reactive
166 group (warhead) of N3 β 1 is identical to that of LW124 and the warhead of N3 β 5 is identical to that of
167 MVB127 (**Figures 1a** and **2a**). Pre-incubation with N3 β 1 suppresses labeling of only the bottom band
168 3 in the MVB072 labeling profile, confirming that this inhibitor is selective for the β 1 subunit (**Figure**
169 **2b**, lane 2). By contrast, pre-incubation with N3 β 5 suppresses MVB072 labeling of the middle band 2,
170 confirming selectivity for β 5 (**Figure 2b**, lane 3).

171 Having verified the selectivity of N3 β 1 and N3 β 5, we tested if LW124 and MVB127 labeling
172 can be suppressed by the respective subunit-selective inhibitor. N3 β 1 suppresses labeling of LW124
173 (**Figure 2b**, lanes 5 and 8), confirming that LW124 targets β 1, consistent with the structural similarity
174 of LW124 with N3 β 1 (**Figures 1a** and **2a**). Importantly, the suppression of MVB127 labeling by N3 β 5
175 (**Figure 2b**, lanes 6 and 12) shows that MVB127 targets β 5, consistent with the structural similarity of
176 MVB127 with N3 β 5 (**Figures 1a** and **2a**). The β 5-MVB127 conjugate (band 5) migrates slightly faster
177 in the protein gel than the β 5-MVB072 conjugate (band 2), consistent with the different MW of the
178 two probes (**Figures 1b** and **1c**, lanes 1 & 3, and **2b**, lanes 1 & 4). Importantly, pre-incubation of
179 N3 β 1 or N3 β 5 in the reciprocal combinations with the probes, did only slightly reduce MVB127 and
180 LW124 labeling, respectively (**Figure 2b**, lanes 5, 6, 9, and 11), indicating that both inhibitors and
181 probes are specific for their targets. Taken together these data show that LW124 and MVB127 are
182 selective probes for β 1 and β 5 catalytic subunits, respectively.

183

184 *Specific labeling of the β 2 catalytic subunit*

185 Having established selective labeling of the $\beta 1$ and $\beta 5$ catalytic subunits, we next developed a method
186 to monitor $\beta 2$. We previously found that RhSylA targets the proteasome subunits $\beta 2$ and $\beta 5$ at short
187 labeling times (Kolodziejek et al., 2011). Taking advantage of this feature we tested if inhibition of the
188 $\beta 5$ proteasome subunit using N3 $\beta 5$ together with short labeling by RhSylA will result in specific
189 labeling of $\beta 2$. We therefore pre-incubated Arabidopsis leaf extracts with various concentrations of
190 N3 $\beta 5$ and labeled for 30 min with 0.5 μM RhSylA. Increasing N3 $\beta 5$ concentrations up to 5 μM N3 $\beta 5$
191 reduces $\beta 5$ labeling (**Figures 3a** and **3b**). $\beta 5$ labeling remains unaltered at higher N3 $\beta 5$ concentrations
192 (**Figures 3a** and **3b**) indicating that $\beta 5$ subunit is saturated by N3 $\beta 5$. Signal intensities derived from $\beta 1$
193 and $\beta 5$ at 5 μM N3 $\beta 5$ are very faint in comparison to the $\beta 2$ signal, which remains unaffected (**Figure**
194 **3b**). This data demonstrates that RhSylA labeling in the presence of 5 μM N3 $\beta 5$ is a suitable approach
195 to monitor labeling of $\beta 2$.

196

197 *Subunit-specific probes display multiple $\beta 1$ signals in *N. benthamiana**

198 *N. benthamiana* is increasingly used as a model plant to study protein regulation and localization upon
199 transient expression. Additionally, *N. benthamiana* can be infected by a range of different pathogens,
200 which makes this species ideal to unravel plant defense (Goodin et al., 2008). Labeling of *N.*
201 *benthamiana* leaf extracts with MVB072 results in two signals: one strong signal at 28 kDa and one
202 faint signal at ca. 27 kDa (**Figure 4a**, lane 1, bands 1 and 2, Misas-Villamil et al., 2013). MS analysis
203 of the MVB072-labeled proteins representing the major signal revealed that it contains $\beta 1$, $\beta 2$ and $\beta 5$
204 subunits (Misas-Villamil et al., 2013). Thus, in contrast to Arabidopsis where the three catalytic
205 subunits cause three distinct signals, the *N. benthamiana* proteasome subunits cannot be distinguished
206 by MVB072 labeling because the signals overlap.

207 To monitor the catalytic subunits of the *N. benthamiana* proteasome, we tested the subunit-
208 selective probes. Surprisingly, LW124 labeling displays two 27 kDa signals, indicating that there
209 might be two different subunits labeled by LW124 in *N. benthamiana* (**Figure 4a**, lane 2, bands 3 and
210 4). Co-labeling of MVB072 with LW124 shows two signals for LW124 and one signal for MVB072
211 (**Figure 4a**, lane 4 overlay). The weak bottom MVB072 signal (band 2) is absent upon co-labeling
212 with LW124, indicating that this signal is caused by $\beta 1$. Because the top MVB072 signal (band 1) also
213 contains $\beta 1$ (Misas-Villamil et al., 2013), both MVB072 signals contain $\beta 1$, consistent with the two
214 signals displayed by LW124. The overlay, however, shows that the two MVB072 signals migrate
215 slower in the gel than the two LW124 conjugates (**Figure 4a**, lanes 1 and 2), which is consistent with
216 the MW shift seen for Arabidopsis, and is explained from the fact that MVB072 is larger and more
217 bulkier when compared to LW124 (**Figures 1a** and **2a**).

218 MVB127 labeling shows one specific signal at 28 kDa (**Figure 4a**, lane 3, band 5). Co-
219 labeling of MVB072 with MVB127 causes a more intense bottom signal, caused by an overlap of the
220 $\beta 1$ -MVB072 and $\beta 5$ -MVB127 conjugates. The observation that the $\beta 5$ -MVB127 conjugate migrates
221 faster through the protein gel than the $\beta 5$ -MVB127 conjugate is consistent with the MW shift seen for

222 Arabidopsis, and is explained from the fact that MVB072 is larger and more bulkier when compared
223 to MVB127 (**Figures 1a** and **2a**). LW124 and MVB127 co-labeling results in two signals for LW124
224 and one signal for MVB127 (**Figure 4a**, lane 6).

225 Pre-incubation with N3 β 1 and N3 β 5 confirms that the lowest MVB072 signal (**Figure 4b**,
226 band 2) and the two LW124 correspond to β 1 (**Figure 4b**, bands 3 and 4), whereas the MVB127 signal
227 corresponds to β 5 (**Figure 4b**, band 5), supporting the specificity of β 1 and β 5 labeling by LW124 and
228 MVB127, respectively (**Figure 4b**, lanes 5-12). There is, however, some reciprocal suppression of
229 N3 β 1 on MVB127(β 5) and N3 β 5 on LW124(β 5) (**Figure 4b**, lanes 5, 6, 9 and 11).

230

231 *Phylogenetic and proteomic analysis reveals multiple incorporated proteasome subunits in N.*
232 *benthamiana*

233 The detection of two β 1 signals in *N. benthamiana* using LW124 is remarkable, since the Arabidopsis
234 genome has only one gene encoding β 1, and *β 1din* in tobacco is defence induced (Suty et al., 2003).
235 We therefore searched the *N. benthamiana* genome (<https://solgenomics.net/>) for genes encoding
236 catalytic subunits of the proteasome. Blast searches for catalytic subunits resulted in six predicted β 1
237 proteins, three β 2 proteins and three β 5 proteins. Phylogenetic analysis revealed that the paralogous
238 subunits are more related to each other than to the subunits of Arabidopsis, except for β 1, where two
239 groups seem to exist in *N. benthamiana* (**Figure 5**). One β 1 and one β 2 subunit are shorter than their
240 respective paralogs. We consider these pseudogenes since their predicted MW is too low to explain the
241 signals we detect upon labeling.

242 To determine if these genes also encode for proteins that are part of the active proteasome in
243 leaves, we performed mass spectrometry analysis of two different pull down experiments of *N.*
244 *benthamiana* leaf extracts labeled with MVB072. To also detect an altered subunit assembly during
245 defence, the pull down was performed on plants treated with the SA analog benzothiadiazole (BTH),
246 whereas the other pull down was performed on the mock control. Each pull down assay was analyzed
247 twice by MS and 45 peptides were detected of the catalytic subunits, of which 11 were unique
248 (Supplemental **Table S1** and **Figure S3**).

249 In these experiments we identified unique peptides of two different β 1 subunits: β 1a and β 1b
250 (**Figures 5b**, **5c** and **S2**). Several peptides that are shared with one other protein (dark grey) map to the
251 truncated β 1 subunit (NbS00011733g0005.1) (dark grey in **Figure 5c**). The truncated subunit would
252 migrate at a predicted 16.7 kDa, but we do not detect fluorescent signals in this region. Removal of
253 this subunit from the analysis would add two additional unique peptides to one of the already
254 identified β 1a subunit (NbS0009991g0103.1). The presence of two β 1 subunits having a different
255 predicted MW of 23.7 (β 1a) and 22.6 (β 1b) kDa is consistent with the two LW124 signals detected
256 upon labeling.

257 We also detected unique peptides for two β 2 subunits (β 2a and β 2b) and one β 5 subunit (β 5a)
258 (**Figure 5b**). Two other β 5 subunit peptides do not match to this identified β 5a protein, indicating that

259 there must be a second $\beta 5$ subunit ($\beta 5b$), which is either Nb00003340g0007.1 or the shorter
260 NbS00002498g0003.1 (**Figures 5b** and **5c**). These findings confirm an expanded repertoire of
261 catalytic proteasome subunits in active proteasomes of *N. benthamiana*.

262 Comparison of the identified proteasome subunits from water- and BTH-treated plants did not
263 reveal significant differences (**Figure 5b**). These data suggest that the active catalytic proteasome
264 subunit incorporation is not different during SA-induced defence. However, more quantitative
265 proteomic analysis with more samples may be required to rule out any changes upon BTH treatment.

266

267 *Bacterial infections affect active subunit composition in N. benthamiana.*

268 We next used the subunit-selective probes to investigate changes in the proteasome subunit
269 composition during biotic stress. We therefore infected *N. benthamiana* leaves with *P. syringae* pv.
270 *tomato* DC3000 (PtoDC3000), which triggers a non-host response (NHR, or effector-triggered
271 immunity (ETI)) because it produces type-III effector hopQ1-1, which is recognized in *N.*
272 *benthamiana*. We also included the Δ hopQ1-1 mutant of PtoDC3000 (PtoDC3000(Δ hQ)), which
273 causes disease on *N. benthamiana* (Wei et al., 2007).

274 Unexpectedly, whilst the proteasome labeling upon infection with PtoDC3000(Δ hQ) is highly
275 reproducible, we noticed that proteasome labeling upon infection with PtoDC3000(WT) differs
276 significantly between eight independent infection assays. MVB072 labeling of extracts of
277 PtoDC3000(WT)-infected leaves indicates that the activity of the proteasome is either upregulated
278 (**Figure 6a**), or down regulated (**Figure 6b**). Importantly, labeling the same extracts with
279 LW124+MVB127, provides much more insight. The lower $\beta 1$ signal either intensifies strongly upon
280 PtoDC3000(WT) infection (**Figure 6c**, Supplemental **Figures S4-S5**), or only slightly (**Figure 6d**,
281 Supplemental **Figures S6-S8**). Remarkably, however, the $\beta 5$ signal is either induced (**Figure 6c**,
282 Supplemental **Figures S4-S5**) or strongly suppressed (**Figure 6d**, Supplemental **Figures S6-S8**). The
283 fact that the ratio between $\beta 1$ and $\beta 5$ can differ between infection experiments significantly
284 demonstrates that the activities of these two subunits can be uncoupled during bacterial infection. The
285 cause of this phenotypic variation upon PtoDC3000(WT) infection is beyond the focus of the current
286 manuscript, and is subject to further studies.

287 Proteasome activities upon infection by PtoDC3000(Δ hQ) show a robust 3-fold upregulation
288 in the intensity of the $\beta 1$ and $\beta 5$ signals (**Figure 6e**, Supplemental **Figure S9**). Quantitative RT-PCR
289 with gene-specific primers showed that also transcript levels of $\beta 1a$, $\beta 1b$ and $\beta 5$ are significantly
290 upregulated (**Figure 6f**), indicating that the differential proteasome activity upon PtoDC3000(Δ hQ) is
291 mostly transcriptional. Notably, we detect a highly reproducible shift in the ratio between the two $\beta 1$
292 signals upon infection with PtoDC3000(Δ hQ) (**Figure 6g**).

293

294 **DISCUSSION**

295 We have introduced next generation subunit-specific probes for labeling the $\beta 1$ and $\beta 5$ proteasome
296 catalytic subunits, and validated labeling in both *Arabidopsis thaliana* and *Nicotiana benthamiana*.
297 We also introduced and validated subunit-selective inhibitors for the $\beta 1$ and $\beta 5$ subunits, which may
298 be useful for chemical knockout assays. We discovered that the active *N. benthamiana* proteasome
299 contains different paralogous catalytic subunits: two for $\beta 1$, two for $\beta 2$ and two for $\beta 5$. Application of
300 selective subunit labeling revealed and uncoupled induction in $\beta 1$ and $\beta 5$ subunits upon infection with
301 virulent and avirulent *Pseudomonas syringae*.

302 Our data demonstrate that LW124 targets $\beta 1$ and MVB127 targets $\beta 5$. Because the proteasome
303 subunits of *Arabidopsis* have a distinct MW, we would have detected additional signals if LW124 and
304 MVB127 would label additional catalytic subunits. Likewise, MVB127 should have caused an
305 additional signal if it could label $\beta 1$ of *N. benthamiana*. The absence of additional signals in
306 *Arabidopsis* testifies the high selectivity of the subunit-selective probes.

307 By contrast, however, despite their structural similarity with the probes, the subunit-selective
308 inhibitors partially suppress reciprocal labeling: N3 $\beta 1$ suppresses labeling of $\beta 5$ by MVB127 and
309 N3 $\beta 5$ suppresses labeling by LW124, in both *Arabidopsis* (**Figure 2b**) and *N. benthamiana* (**Figure**
310 **4b**). Likewise, we detect a consistent suppression of $\beta 5$ labeling by MVB127 upon colabeling with
311 LW124 (**Figures 1c, 2b, 4a and 4b**). Although we can not exclude at this stage that N3 $\beta 1$ and N3 $\beta 5$
312 are weak inhibitors of $\beta 5$ and $\beta 1$, respectively, the fact that the corresponding probes are subunit
313 selective suggest an alternative explanation. The suppression of labeling by inhibitors and probes that
314 target other subunits may also be caused by crowding of the proteolytic chamber (inhibitor bound to
315 one subunit hinders access of probes to another subunit) or allosteric regulation (inhibition of one
316 subunits affects labeling efficiency of another subunit). Although the proteolytic chamber is probably
317 too large to support the crowded chamber hypothesis, the catalytic subunits of the proteasome are
318 known to allosterically regulate each other, e.g. to facilitate the cyclical bite-chew mechanism
319 (Kisselev et al., 1999).

320

321 *N. benthamiana* assembles different proteasomes

322 LW124 labeling of *N. benthamiana* displays two different $\beta 1$ signals. MS analysis of MVB072 labeled
323 proteins confirmed that at least two different $\beta 1$ proteins are incorporated in proteasomes as active
324 catalytic subunits. Subunits that are not incorporated into the proteasome remain in the inactive
325 precursor state and are probably degraded (Chen & Hochstrasser, 1996). MS analysis of MVB072-
326 labeled proteins also revealed at least two different $\beta 2$ proteins and two different $\beta 5$ subunits that must
327 have been part of an active proteasome. However, MVB127 labeling only displays one $\beta 5$ signal,
328 indicating that the labeled proteins run at the same height. The fact that multiple paralogs were
329 identified demonstrates that *N. benthamiana* produces diverse catalytic subunits and might assemble
330 different proteasomes.

331 The concept that plants can assemble multiple proteasomes is supported by the finding that
332 Arabidopsis also incorporates paralogous subunits into the 26S proteasome (Yang et al., 2004; Book et
333 al., 2010). Remarkably, little is known about the role of paralogous CP subunits but more about
334 paralogous RP subunits. Different paralogs of a subunit may act redundantly. For example, the RPN1
335 subunit in Arabidopsis is encoded by two genes, *RPN1a* and *RPN1b*, which differ in their expression
336 pattern (Yang et al., 2004). Nevertheless, *rpn1a* mutant lines maintain a functional proteasome
337 indicating a redundant function (Wang et al., 2009). RPT2 and RPT5 isoforms also share redundant
338 functions (Lee et al., 2011). In both Arabidopsis and maize, RPT2 and RPT5 are encoded by the
339 paralogous genes *RPT2a - RPT2b* and *RPT5a - RPT5b*, respectively (Book et al., 2010). However,
340 there are cases where paralogous subunits seem to have different functions. For example, *RPT5b*
341 complements *RPT5a* in the *Col* ecotype, but not in *Ws* ecotype (Gallois et al., 2009), demonstrating an
342 ecotype-dependent redundancy but also indicating alternative functions for the different isoforms. *N.*
343 *benthamiana* is an allotetraploid, and the ancient genome duplication may explain a duplication of the
344 proteasome subunits genes. At this stage, it is unclear if the different paralogous proteins have
345 different functions.

346

347 *Modification of the proteasome upon bacterial infection.*

348 Interestingly, subunit-selective proteasome activity profiling revealed that the activity of the catalytic
349 $\beta 5$ subunit can be strongly induced or suppressed upon infection with *Pseudomonas syringae* and
350 show that the activities of $\beta 1$ and $\beta 5$ can be uncoupled during infection. Uncoupling is not expected
351 for proteasome complexes that incorporate equal numbers of catalytic subunits, but may have been
352 caused by selective subunit inhibition during infection with *P. syringae*, or the specific activation of
353 the $\beta 1$ subunit during NHR/ETI responses.

354 Mammals have inducible subunits that can replace other β subunits, e.g. to create the
355 immunoproteasome (Aki et al., 1994). Immunoproteasomes exhibit modified peptidase activities and
356 variable cleavage site preferences. Their main function is the maintenance of cell homeostasis and cell
357 viability under oxidative conditions (Seifert et al., 2010). It is likely that plants also possess a type of
358 inducible proteasome where some catalytic subunits are replaced under biotic or abiotic stresses. We
359 have identified six genes encoding $\beta 1$ catalytic subunits from the *N. benthamiana* genome, suggesting
360 that the other isoforms that we did not detect by MS analysis are either expressed under different
361 conditions, are tissue specific or are pseudogenes. This can also be the case for non identified $\beta 2$ and
362 $\beta 5$ proteins. Induction of genes encoding α and β proteasome subunits has been described for tobacco
363 cells treated with cryptogein (Dahan et al., 2001), whereas our earlier study revealed a post-
364 translational upregulation of proteasome labeling upon treatment of Arabidopsis with benzodiazole
365 (Gu et al., 2010). Transcript activation of proteasome genes after cryptogein treatment could be
366 associated with oxidative stress, since attenuation of the oxidative burst blocks the expression of
367 *$\beta 1din$* , *$\alpha 3din$* and *$\alpha 6din$* genes (Suty et al., 2003).

368 Thus, different paralogous proteasome subunits might be assembled in active proteasomes
369 under different conditions, for instance responding to oxidative stress. The encoded catalytic subunits
370 in *N. benthamiana* carry only few polymorphic amino acid residues, and it is unknown at this stage to
371 what extent they affect proteasome function, e.g. with respect to substrate selection and conversion.
372 This study uncovers that more research is needed to investigate the occurrence and function of
373 alternative proteasomes in plants.

374 Taken together, we have introduced subunit-specific probes to monitor the $\beta 1$ and $\beta 5$ subunits
375 of the plant proteasome. The use of site-specific probes combined with phylogenetic and proteomic
376 analysis revealed multiple isoforms for the β subunits, indicating that different proteasomes co-exist in
377 leaves. The subunit selective probes revealed unexpected, uncoupled differential activities of $\beta 1$ and
378 $\beta 5$ upon bacterial infection, that raise exciting questions on the underlying mechanism and biological
379 role in immunity.

380

381

382 **EXPERIMENTAL PROCEDURES**

383 *Probes and inhibitors*

384 The synthesis of LW124, MVB127, N3 $\beta 1$ and N3 $\beta 5$ has been described previously (Verdoes et al.,
385 2010; Li et al., 2013). As with our previously introduced probes, aliquots of these chemicals are
386 available upon request and frequent use may accelerate their commercial availability.

387

388 *Plant material and labeling conditions*

389 *Arabidopsis thaliana* ecotype Col-0 and *Nicotiana benthamiana* plants were grown in the greenhouse
390 under a regime of 14 h light at 20 °C. 3–5 weeks old plants were used for labeling experiments. For *in*
391 *vitro* labeling, leaves were ground in water containing 10 mM DTT and extracts were cleared by
392 centrifugation. Labeling was performed by incubating the protein extract in 60 μ l buffer containing
393 66.7 mM Tris pH 7.5 and 0.5 – 0.8 μ M probe for 2 h at room temperature (22–25 °C) in the dark.
394 After acetone precipitation pellets were re-suspended in 40 μ l 1x loading buffer and samples were
395 separated on 12% SDS gel. Inhibitory assays were performed by 30 min pre-incubation of protein
396 extracts with 50 μ M of the inhibitor of interest, followed by 2 h labeling. For *in vivo* inhibition of the
397 proteasome 50 μ M of the inhibitor was infiltrated in *N. benthamiana* leaves using a syringe without a
398 needle. After 6 h incubation at room temperature, a leaf disc (1.6 cm diameter) of the infiltrated area
399 was collected and labeled with the probe of interest as described above. Labeled proteins were
400 visualized by in-gel fluorescence scanning using a Typhoon FLA 9000 scanner (GE Healthcare,
401 <http://www.gelifesciences.com>) with Ex473/Em530 nm for LW124 and Ex532/Em580 nm for
402 MVB127, MVB072 and RhSylA. Fluorescent signals were quantified using ImageQuant 5.2 (GE
403 Healthcare) with the rolling ball method for background correction. To confirm equal loading,
404 Coomassie brilliant blue or SyproRuby (Invitrogen) staining was performed according to the

405 instructions of the manufacturer. SyproRuby gels were fluorescent scanned (Ex472/Em580 nm) and
406 used for loading correction in the quantification of fluorescent signals. Statistical significance was
407 calculated with a student's t-test of at least three replicates.

408

409 *Large scale pull down assay*

410 Large scale pull down experiments were performed once on plants treated with benzothiadiazole
411 (BTH) and once on the water control. This material was generated by spraying 3-4-week old *N.*
412 *benthamiana* plants with 0.13 mg/mL BTH (BION, Syngenta) containing 0.01% Silwet L-77 (Lehle
413 Seeds) or sprayed with water containing the same concentration of Silwet L-77. Leaves were
414 harvested two days after treatment. 44 leaf discs of 2.3 cm diameter were collected per sample and
415 ground in a buffer containing 1 mM DTT and 67 mM Tris pH 7.5. After centrifugation, 10 ml of
416 protein extract was used for labeling with 20 μ M MVB072 or 2.5 μ l DMSO. Samples were incubated
417 at room temperature and in the dark with gentle shaking for 2 h. Labeling was stopped by precipitating
418 total proteins via the chloroform/methanol precipitation method (Wessel and Flügge, 1984). Affinity
419 purification and in-gel digestion was performed as described elsewhere (Chandrasekar et al., 2014).

420

421 *Mass spectrometry*

422 LC-MS/MS Experiments were performed on an Orbitrap Elite instrument (Thermo, Michalski et al.
423 2012) that was coupled to an EASY-nLC 1000 liquid chromatography (LC) system (Thermo). The LC
424 was operated in the one-column mode. The analytical column was a fused silica capillary (75 μ m \times 15
425 cm) with an integrated PicoFrit emitter (New Objective) packed in-house with Reprosil-Pur 120 C18-
426 AQ 1.9 μ m resin (Dr. Maisch). The LC was equipped with two mobile phases: solvent A (0.1% formic
427 acid, FA, in water) and solvent B (0.1% FA in acetonitrile, ACN). All solvents were of UPLC grade
428 (Sigma). Peptides were directly loaded onto the analytical column with a maximum flow rate that
429 would not exceed the set pressure limit of 800 bar (usually around 0.7 – 0.8 μ l/min). Peptides were
430 subsequently separated on the analytical column by running a 60 min or 120 min gradient of solvent A
431 and solvent B (60 min runs: start with 2% B; gradient 2% to 10% B for 2.5 min; gradient 10% to 35%
432 B for 45 min; gradient 35% to 45% B for 7.5 min; gradient 45% to 100% B for 2 min and 100% B for
433 3 min. 120 min runs: start with 2% B; gradient 2% to 10% B for 5 min; gradient 10% to 35% B for 90
434 min; gradient 35% to 45% B for 15 min; gradient 45% to 100% B for 4 min and 100% B for 6 min.) at
435 a flow rate of 300 nl/min. The mass spectrometer was operated using Xcalibur software (version 2.2
436 SP1.48). The mass spectrometer was set in the positive ion mode. Precursor ion scanning was
437 performed in the Orbitrap analyzer (FTMS) in the scan range of m/z 300-1800 and at a resolution of
438 60000 with the internal lock mass option turned on (lock mass was 445.120025 m/z , polysiloxane)
439 (Olsen et al., 2005). Product ion spectra were recorded in a data dependent fashion in the ion trap
440 (ITMS) in a variable scan range and at a rapid scan rate. The ionization potential (spray voltage) was
441 set to 1.8 kV. Peptides were analyzed using a repeating cycle consisting of a full precursor ion scan

442 (1.0 × 10⁶ ions or 200 ms) followed by 15 product ion scans (1.0 × 10⁴ ions or 50 ms) where peptides
443 are isolated based on their intensity in the full survey scan (threshold of 500 counts) for tandem mass
444 spectrum (MS2) generation that permits peptide sequencing and identification. CID collision energy
445 was set to 35% for the generation of MS2 spectra. For the 2 h gradient length the data dependent
446 decision tree option and supplemental activation was switched on. The ETD reaction time was 100 ms.
447 During MS2 data acquisition dynamic ion exclusion was set to 30 seconds with a maximum list of
448 excluded ions consisting of 500 members and a repeat count of one. Ion injection, time prediction,
449 preview mode for the FTMS, monoisotopic precursor selection and charge state screening were
450 enabled. Only charge states higher than 1 were considered for fragmentation.

451

452 *Peptide and Protein Identification using MaxQuant*

453 RAW spectra were submitted to an Andromeda (Cox et al., 2011) search in MaxQuant (version
454 1.5.3.30) using the default settings (Cox et al., 2008) Match-between-runs was activated (Cox et al.,
455 2014) MS/MS spectra data were searched against the in-house generated *Nicotiana benthamiana*
456 database (78729 entries). All searches included a contaminants database (as implemented in
457 MaxQuant, 267 sequences). The contaminants database contains known MS contaminants and was
458 included to estimate the level of contamination. Andromeda searches allowed oxidation of methionine
459 residues (16 Da) and acetylation of protein N-terminus (42 Da) as dynamic modification and the static
460 modification of cysteine (57 Da, alkylation with iodoacetamide). Enzyme specificity was set to
461 “Trypsin/P”. The instrument type in Andromeda searches was set to Orbitrap and the precursor mass
462 tolerance was set to ±20 ppm (first search) and ±4.5 ppm (main search). The MS/MS match tolerance
463 was set to ±0.5 Da. The peptide spectrum match FDR and the protein FDR were set to 0.01 (based on
464 target-decoy approach). Minimum peptide length was 7 amino acids. The minimum score for modified
465 peptides was 40.

466

467 *Extraction of proteasome specific peptides*

468 The peptide.txt output files from MaxQuant were loaded into Perseus v1.5.3.0. After removal of
469 peptides matching to the reversed database and peptides matching to the contaminant database the
470 remaining peptides were annotated using an in-house annotation file (annotation.wOG.txt). Peptides
471 annotated to be derived from the proteasome or a proteasome subunit were extracted (Supplementary
472 **Table S1**) and manually mapped to the individual proteasome sequences (Supplementary **Figure S2**).

473

474 *Database search and phylogenetic analysis*

475 The *N. benthamiana* database (v. 0.4.4, 76,379 sequences) was downloaded from the SOL genomics
476 network (<https://solgenomics.net>) and a blast search using Arabidopsis catalytic subunits as a template
477 was performed. Additionally, *N. benthamiana* annotated T1 proteins found in the MEROPS database
478 (<https://merops.sanger.ac.uk>) were compared with the hits obtained by the search with Arabidopsis

479 orthologs. The sequences were aligned with ClustalX2 (Larkin et al., 2007) standalone program. The
480 alignment parameters were used as follows: the pair wise alignment gap opening penalty 30 and gap
481 extension penalty 0.75, whereas for multiple alignment gap opening penalty were set to 15 and gap
482 extension penalty to 0.3. Finally, the output alignment file from the ClustalX2 was used to generate
483 the tree in R (Charif and Lobry, 2007; Paradis et al., 2004). The neighbor-joining algorithm was
484 implemented in the script for the construction of the phylogenetic tree from the calculated distance
485 matrix.

486

487 *Bacterial infections*

488 For *P. syringae* infection, leaves of five-week old *N. benthamiana* plants were infiltrated using a
489 needle-less syringe with 10^6 CFU/mL *Pseudomonas syringae* pv. *tomato* DC3000 and its *ΔhopQ1-1*
490 mutant derivative (Wei et al., 2007). Three leaf discs (d=1 cm) were harvested at days 1 and 2. Leaf
491 extracts were generated in 200 μL of 50 mM Tris buffer at pH 7.5 containing 5 mM DTT, cleared by
492 centrifugation and labeled for two hours with 0.2 μM MVB072 or 0.8 μM LW124 + 0.8 μM MVB127
493 at room temperature in the dark in 50 μL total volume.

494

495 *Nucleic acid preparation, cDNA synthesis and qRT-PCR*

496 For RNA extraction, leaf material of *N. benthamiana* infected leaves was frozen in liquid nitrogen,
497 ground to powder. The RNA was extracted using Trizol (Ambion), treated with DNase (QIAGEN),
498 purified using the RNeasy Plant Mini Kit (QIAGEN) and used the SuperScript™ III Reverse
499 Transcriptase (Invitrogen) for cDNA synthesis. The first-strand cDNA synthesis kit was used to
500 reverse transcribe 1 μg of total RNA with oligo(dT) Primers. The qRT-PCR analysis was performed
501 using the iQ SYBR Green Supermix (Bio-Rad) with an iCycler (Bio-Rad). Specific primers were used
502 to amplify *β1a* (forward: 5'-ctgctggatattgtgcctgc-3', reverse: 5'-ggctcaaacatgctgcagct-3'), *β1b*
503 (forward: 5'-tgcccctattcacgtgttg-3', reverse: 5'-gttcagcaggacaaaagga-3'), *β5b* (forward: 5'-
504 ctcccattctacgtgctca-3', reverse: 5'-ggattgacttgcttagctcac-3') and *PP2A* (forward: 5'-
505 gacctgatgttgatgttcgct-3', reverse: 5'-gagggattgaagagagatttc-3') was used as reference gene for
506 normalization. Cycling conditions were as follows: 3 min at 95°C, followed by 45 cycles of 15 sec at
507 95°C, 15 sec at 60°C and 30 sec at 72°C. After each PCR, the specificity of the amplified product was
508 verified with the melting curves. Gene expression levels for *β1a*, *β1b* and *β5a* were then calculated
509 relative to *PP2A* using the 2-ΔCt (cycle threshold) method (Livak and Schmittgen, 2001). The average
510 expression and the standard deviation of one experiment with four individuals were calculated, and
511 expression of the mock control was set to 1. P values were calculated using a two tails *t*-test with
512 unequal variance. P values <0.0005 were marked with three asterisks.

513

514

515 **ACKNOWLEDGEMENTS**

516 We would like to thank Prof. Gunther Doehleman and Prof. George Coupland for their support. We
517 are grateful to Prof. Collmer for providing the Δ hopQ1-1 mutant of PtoDC3000. This work was
518 financially supported by the Max Planck Society, ERC Consolidator grant (R.H., grant No. 616449
519 ‘GreenProteases’), an ERC starting grant (M.K., grant No. 258413), the Deutsche
520 Forschungsgemeinschaft (M.K., grant no. INST 20876/127-1 FUGG) and the University of Oxford.

521 **REFERENCES**

- 522 **Aki, M., Shimbara, N., Takashina, M., Akiyama, K., Kagawa, S., Tamura, T., Tanahashi, N.,**
523 **Yoshimura, T., Tanaka, K. and Ichihara, A.** (1994) Interferon-gamma induces different subunit
524 organizations and functional diversity of proteasomes. *J. Biochem.* **115**, 257-269.
- 525 **Banfield, M.J.** (2015) Perturbation of host ubiquitin systems by plant pathogen/pest effector proteins.
526 *Cell Microbiol.* **17**, 18-25.
- 527 **Book, A.J., Gladman, N.P., Lee, S.S., Scalf, M., Smith, L.M. and Vierstra, R.D.** (2010) Affinity
528 purification of the Arabidopsis 26S proteasome reveals a diverse array of plant proteolytic complexes.
529 *J. Biol. Chem.* **285**, 25554–25569.
- 530 **Carrión, C.A., Costa, M.L., Martínez, D.E., Mohr, C., Humbeck, K. and Guamet, J.J.** (2013) *In*
531 *vivo* inhibition of cysteine proteases provides evidence for the involvement of 'senescence-associated
532 vacuoles' in chloroplast protein degradation during dark-induced senescence of tobacco leaves. *J. Exp.*
533 *Bot.* **64**, 4967-4980.
- 534 **Chandrasekar, B., Colby, T., Emon, A.E.K., Jiang, J., Hong, T.N., Villamor, J.G., Harzen, A.,**
535 **Overkleeft, H.S. and Van der Hoorn, R.A.L.** (2014) Broad range glycosidase activity profiling. *Mol.*
536 *Cell. Proteomics* **13**, 2787-2800.
- 537 **Charif, D. and Lobry, J.** (2007) SeqinR 1.0–2: a contributed package to the R project for statistical
538 computing devoted to biological sequences retrieval and analysis. In: Structural Approaches to
539 Sequence Evolution (Bastolla U., Porto M., Roman H. E., Vendruscolo M., eds), pp. 207–232,
540 Springer, Berlin
- 541 **Chen, P. and Hochstrasser, M.** (1996) Autocatalytic subunit processing couples active site formation
542 in the 20S proteasome to completion of assembly. *Cell* **86**, 961–972.
- 543 **Cox, J., Hein, M.Y., Lubner, C.A., Paron, I., Nagaraj, N. and Mann, M.** (2014) Accurate Proteome-
544 wide Label-free Quantification by Delayed Normalization and Maximal Peptide Ratio Extraction,
545 Termed MaxLFQ. *Mol. Cell. Proteomics* **13**, 2513-2526.
- 546 **Cox, J. and Mann, M.** (2008) MaxQuant enables high peptide identification rates, individualized
547 p.p.b.-range mass accuracies and proteome-wide protein quantification. *Nat. Biotechnol* **26**, 1367-
548 1372.
- 549 **Cox, J., Neuhauser, N., Michalski, A., Scheltema, R.A., Olsen, J.V. and Mann, M.** (2011)
550 Andromeda: a peptide search engine integrated into the MaxQuant environment. *J. Proteome Res.* **10**,
551 1794-1805.
- 552 **Cravatt, B.F., Wright, A.T. and Kozarich, J.W.** (2008) Activity-based protein profiling: from
553 enzyme chemistry to proteomic chemistry. *Annu. Rev. Biochem.* **77**, 383–414.
- 554 **Dahan, J., Etienne, P., Petitot, A.S., Houot, V., Blein, J.P. and Suty, L.** (2001) Cryptogein affects
555 expression of $\alpha 3f$, $\alpha 6$ and $\beta 1$ proteasome subunits encoding gene in tobacco. *J. Exp. Bot.* **52**, 1947-
556 1948.

557 **Dick, T.P., Nussbaum, A.K., Deeg, M., Heinemeyer, W., Groll, M., Schirle, M., Keilholz, W.,**
558 **Stevanović, S., Wolf, D.H., Huber, R., Rammensee, H.G. and Schild, H.** (1998) Contribution of
559 proteasomal β -subunits to the cleavage of peptide substrates analyzed with yeast mutants. *J. Biol.*
560 *Chem.* **273**, 25637-25646.

561 **Dong, S., Stam, R., Cano, L.M., Song, J., Sklenar, J., Yoshida, K., Bozkurt, T.O., Oliva, R., Liu**
562 **,Z., Tian, M., Win, J., Banfield, M.J., Jones, A.M., Van der Hoorn, R.A.L. and Kamoun, S.**
563 (2014) Effector specialization in a lineage of the Irish potato famine pathogen. *Science* **343**, 552-555.

564 **Gallois, J.L., Guyon-Debast, A., Le´ cureuil, A., Vezon, D., Carpentier, V., Bonhomme, S. and**
565 **Guerche, P.** (2009) The Arabidopsis proteasome RPT5 subunits are essential for gametophyte
566 development and show accession-dependent redundancy. *Plant Cell* **21**, 442-459.

567 **Goodin, M.M., Zaitlin, D., Naidu, R.A. and Lommel, S.A.** (2008) *Nicotiana benthamiana*: Its
568 history and future as a model for plant–pathogen interactions. *Mol. Plant-Microbe Interact.* **21**, 1015-
569 1026.

570 **Greenbaum, D., Medzihradzky, K.F., Burlingame, A. and Bogyo, M.** (2000) Epoxide
571 electrophiles as activity-dependent cysteine protease profiling and discovery tools. *Chem. Biol.* **7**, 569-
572 581.

573 **Groll, M., Ditzel, L., Löwe, J., Stock, D., Bochtler, M., Bartunik, H.D. and Huber, R.** (1997)
574 Structure of 20S proteasome from yeast at 2.4 Å resolution. *Nature* **386**, 463-471.

575 **Groll, M., Schellenberg, B., Bachmann, A.S., Archer, C.R., Huber, R., Powell, T.K., Lindow, S.,**
576 **Kaiser, M. and Dudler, R.** (2008) A plant pathogen virulence factor inhibits the eukaryotic
577 proteasome by a novel mechanism. *Nature* **452**, 755-758.

578 **Gu, C., Kolodziejek, I., Misas-Villamil, J.C., Shindo, T., Colby, T., Verdoes, M., Richau, K.H.,**
579 **Schmidt, J., Overkleef, H.S. and Van der Hoorn, R.A.L.** (2010) Proteasome activity profiling: a
580 simple, robust and versatile method revealing subunit-selective inhibitors and cytoplasmic, defence-
581 induced proteasome activities. *Plant J.* **62**, 160-170.

582 **Gu, C.** (2009) Activity-based protein profiling in plants. PhD Thesis, University of Cologne.

583 **Hörger, A.C., Ilyas, M., Stephan, W., Tellier, A., Van der Hoorn, R.A.L. and Rose, L.E.** (2012)
584 Balancing selection at the tomato RCR3 guardee gene family maintains variation in strength of
585 pathogen defense. *PLoS Genetics* **8**, e1002813.

586 **Kaschani, F., Shabab, M., Bozkurt, T., Shindo, T., Schornack, S., Gu, C., Ilyas, M., Win, J.,**
587 **Kamoun, S. and Van der Hoorn, R.A.L.** (2010) An effector-targeted protease contributes to defense
588 against *Phytophthora infestans* and is under diversifying selection in natural hosts. *Plant Physiol.* **154**,
589 1794-1804.

590 **Kisselev, A. F., Kopian, T. N., Castillo, V., and Goldberg, A. L.** (1999) Proteasome active sites
591 allosterically regulate each other, suggesting a cyclical bite-chew mechanism for protein breakdown.
592 *Mol. Cell* **4**, 395-402.

593 **Kolodziejek, I., Misas-Villamil, J.C., Kaschani, F., Clerc, J., Gu, C., Krahn, D., Niessen, S.,**
594 **Verdoes, M., Willems, L.I., Overkleeft, H.S., Kaiser, M. and Van der Hoorn, R.A.L.** (2011)
595 Proteasome activity imaging and profiling characterizes bacterial effector Syringolin A. *Plant Physiol.*
596 **155**, 477-489.

597 **Kurepa, J. and Smalle, J.A.** (2008a) Structure, function and regulation of plant proteasomes.
598 *Biochimie* **90**, 324-335.

599 **Larkin, M.A., Blackshields, G., Brown, N.P., Chenna, R., McGettigan, P.A., McWilliam, H.,**
600 **Valentin, F., Wallace, I.M., Wilm, A., Lopez, R., Thompson, J.D., Gibson, T.J. and Higgins, D.G.**
601 (2007) Clustal W and Clustal X version 2.0. *Bioinformatics* **23**, 2947-2948.

602 **Lee, K.H., Minami, A., Marshall, R.S., Book, A.J., Farmer, L.M., Walker, J.M. and Vierstra,**
603 **R.D.** (2011) The RPT2 subunit of the 26S proteasome directs complex assembly, histone dynamics,
604 and gametophyte and sporophyte development in Arabidopsis. *Plant Cell* **23**, 4298-4317.

605 **Li, N., Kuo, C.L., Paniagua, G., van den Elst, H., Verdoes, M., Willems, L.I., Van der Linden,**
606 **W.A., Ruben, M., Van Genderen, E., Gubbens, J., Van Wezel, G.P., Overkleeft, H.S. and Florea,**
607 **B.I.** (2013) Relative quantification of proteasome activity by activity-based protein profiling and LC-
608 MS/MS. *Nat. Protocols* **8**, 1155-1168.

609 **Livak K.J. and Schmittgen, T.D.** (2001) Analysis of relative gene expression data using real-time
610 quantitative PCR and the 2(-Delta Delta C(T)) Method. *Methods*. **25**, 402-408.

611 **Martínez, D.E., Bartoli, C.G., Grbic, V. and Guamet, J.J.** (2007) Vacuolar cysteine proteases of
612 wheat (*Triticum aestivum* L.) are common to leaf senescence induced by different factors. *J. Exp. Bot.*
613 **58**, 1099-1107.

614 **Michalski, A., Damoc, E., Lange, O., Denisov, E., Nolting, D., Muller, M., Viner, R., Schwartz,**
615 **J., Belford, M., Dunyach, J.J., Cox, J., Horning, S., Mann, M. and Makarov, A.** (2012) Ultra high
616 resolution linear ion trap Orbitrap mass spectrometer (Orbitrap Elite) facilitates top down LC MS/MS
617 and versatile peptide fragmentation modes. *Mol. Cell. Proteomics* **11**, O111.013698.

618 **Misas-Villamil, J.C., Kolodziejek, I., Crabill, E., Kaschani, F., Niessen, S., Shindo, T., Kaiser,**
619 **M., Alfano, J.R. and Van der Hoorn, R.A.L.** (2013) *Pseudomonas syringae* pv. *syringae* uses
620 proteasome inhibitor Syringolin A to colonize from wound infection sites. *PLoS Pathogens* **9**,
621 e1003281.

622 **Morimoto, K. and Van der Hoorn, R.A.L.** (2016) The increasing impact of activity-based protein
623 profiling in plant science. *Plant Cell Physiol.* **57**, 446-461.

624 **Mueller, A.N., Ziemann, S., Treitschke, S., Aßmann, D. and Doehlemann, G.** (2013)
625 Compatibility in the *Ustilago maydis*-maize interaction requires inhibition of host cysteine proteases
626 by the fungal effector Pit2. *PLoS Pathog.* **9**, e1003177.

627 **Nguyen, H. M., Schippers, J. H., Goni-Ramos, O., Christoph, M. P., Dortay, H., Van der Hoorn,**
628 **R. A. L., and Mueller-Roeber, B.** (2013) An upstream regulator of the 26S proteasome modulates
629 organ size in *Arabidopsis thaliana*. *Plant J.* **74**, 25-36.

630 **Olsen, J.V., de Godoy, L.M., Li, G., Macek, B., Mortensen, P., Pesch, R., Makarov, A., Lange,**
631 **O., Horning, S. and Mann, M.** (2005) Parts per million mass accuracy on an Orbitrap mass
632 spectrometer via lock mass injection into a C-trap. *Mol. Cell. Proteomics* **4**, 2010-2021.

633 **Padmanabhan, A., Vuong, S.A. and Hochstrasser, M.** (2016) Assembly of an evolutionary
634 conserved alternative proteasome isoform in human cells. *Cell Rep.* **14**, 2962-2974.

635 **Paradis, E., Claude, J. and Strimmer, K.** (2004) APE: analyses of phylogenetics and evolution in R
636 language. *Bioinformatics* **20**, 289-290.

637 **Poret, M., Chandrasekar, B., Van der Hoorn, R.A.L. and Avice, J.B.** (2016) Characterization of
638 senescence-associated protease activities in the efficient protein remobilization during leaf senescence
639 of winter oilseed rape. *Plant Sci.* **246**, 139-153.

640 **Rooney, H., Van 't Klooster, J., Van der Hoorn, R.A.L., Joosten, M.H.A.J., Jones, J.D.G. and De**
641 **Wit, P.J.G.M.** (2005) Cladosporium Avr2 inhibits tomato Rcr3 protease required for Cf-2-dependent
642 disease resistance. *Science* **308**, 1783-1789.

643 **Schellenberg B., Ramel, C. and Dudler, R.** (2010) *Pseudomonas syringae* virulence factor
644 Syringolin A counteracts stomatal immunity by proteasome inhibition. *Mol. Plant-Microbe Interact.*
645 **23**, 1287-1293.

646 **Seifert, U., Bialy, L.P., Ebstein, F., Bech-Otschir, D., Voigt, A., Schröter, F., Prozorovski, T.,**
647 **Lange, N., Steffen, J., Rieger, M., Kuckelkorn, U., Aktas, O., Kloetzel, P.M. and Krüger, E.**
648 (2010) Immuno-proteasomes preserve protein homeostasis upon interferon-induced oxidative stress.
649 *Cell* **142**, 613-624.

650 **Shabab, M., Shindo, T., Gu, C., Kaschani, F., Pansuriya, T., Chintha, R., Harzen, A., Colby, T.,**
651 **Kamoun, S. and Van der Hoorn, R.A.L.** (2008) Fungal effector protein AVR2 targets diversifying
652 defence-related Cys proteases of tomato. *Plant Cell* **20**, 1169-1183.

653 **Song, J., Win, J., Tian, M., Schornack, S., Kaschani, F., Muhammad, I., Van der Hoorn, RAL.**
654 **and Kamoun, S.** (2009) Apoplastic effectors secreted by two unrelated eukaryotic plant pathogens
655 target the tomato defense protease Rcr3. *Proc. Natl. Acad. Sci. USA* **106**, 1654-1659.

656 **Suty, L., Lequeu, J., Lancon, A., Etienne, P., Petitot, A.S. and Blein, J.P.** (2003) Preferential
657 induction of 20S proteasome subunits during elicitation of plant defense reactions: towards the
658 characterization of plant defense proteasomes. *Int. J. Biochem. Cell. Biol.* **35**, 637-650.

659 **Tian, M., Win, J., Song, J., Van der Hoorn, R.A.L., Van der Knaap, E. and Kamoun, S.** (2007) A
660 *Phytophthora infestans* cystatin-like protein interacts with and inhibits a tomato papain-like apoplastic
661 protease. *Plant Physiol.* **143**, 364-277.

662 **Üstün, S., Bartetzo, V. and Bornke, F.** (2013) The *Xanthomonas campestris* type III effector XopJ
663 targets the host cell proteasome to suppress salicylic-acid mediated plant defence. *PLoS Pathog.* **9**,
664 e1003427.

665 **Üstün, S., König, P., Guttman, D.S. and Börnke, F.** (2014) HopZ4 from *Pseudomonas syringae*, a
666 member of the HopZ type III effector family from the YopJ superfamily, inhibits the proteasome in
667 plants. *Mol. Plant-Microbe Interact.* **27**, 611-623.

668 **Üstün S, Sheikh A, Gimenez-Ibanez S, Jones A, Ntoukakis V, Börnke F.** (2016) The proteasome
669 acts as a hub for plant immunity and is targeted by *Pseudomonas* type III effectors. *Plant Physiol.* **172**,
670 1941-1958.

671 **Van der Hoorn, R.A.L., Leeuwenburgh, M.A., Bogyo, M., Joosten, M.H.A.J. and Peck, S.C.**
672 (2004) Activity profiling of papain-like cysteine proteases in plants. *Plant Physiol.* **135**, 1170-1178.

673 **Van Esse, H.P., Van't Klooster, J.W., Bolton, M.D., Yadeta, K.A., Van Baarlen, P, Boeren, S.,**
674 **Vervoort, J., De Wit, P.J.G.M. and Thomma, B.P.H.J.** (2008) The *Cladosporium fulvum* virulence
675 protein Avr2 inhibits host proteases required for basal defense. *Plant Cell* **20**, 1948-1963.

676 **Verdoes, M., Willems, L.I., Van der Linden, W.A., Duivenvoorden, B.A., Van der Marel, G.A.,**
677 **Florea, B.I., Kisselev, A.F. and Overkleeft, H.S.** (2010) A panel of subunit-selective activity-based
678 proteasome probes. *Org. Biomol. Chem.* **8**, 2719-2727.

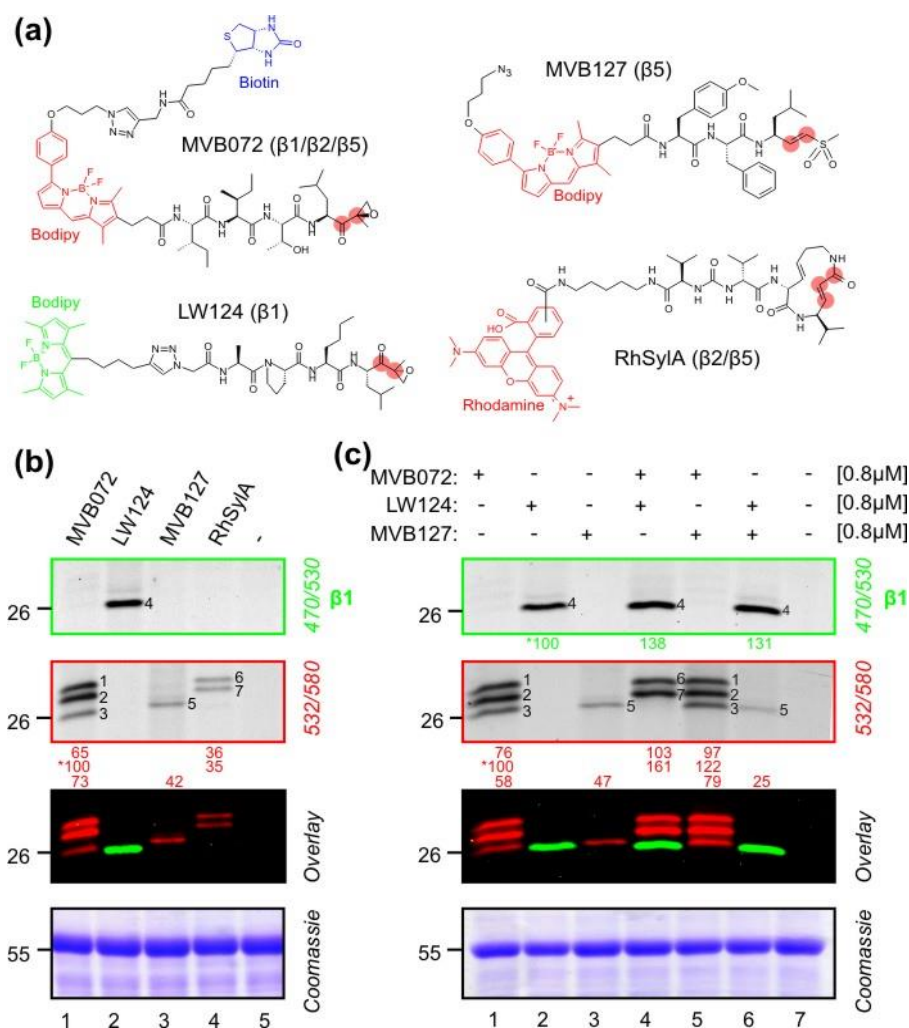
679 **Wang, S., Kurepa, J. and Smalle, J.A.** (2009) The Arabidopsis 26S proteasome subunit RPN1a is
680 required for optimal plant growth and stress responses. *Plant Cell Physiol.* **50**, 1721-1725.

681 **Wei, C.F., Kvitko, B.H., Shimizu, R., Crabill, E., Alfano, J.R., Lin, N.C., Martin, G.B., Huang,**
682 **H.C. and Collmer, A.** (2007) A *Pseudomonas syringae* pv. *tomato* DC3000 mutant lacking the type
683 III effector HopQ1-1 is able to cause disease in the model plant *Nicotiana benthamiana*. *Plant J.* **51**,
684 32-46.

685 **Wessel, D. and Flügel, U.I.** (1984) A method for the quantitative recovery of protein in dilute-
686 solution in the presence of detergents and lipids. *Anal. Biochem.* **138**, 141-143.

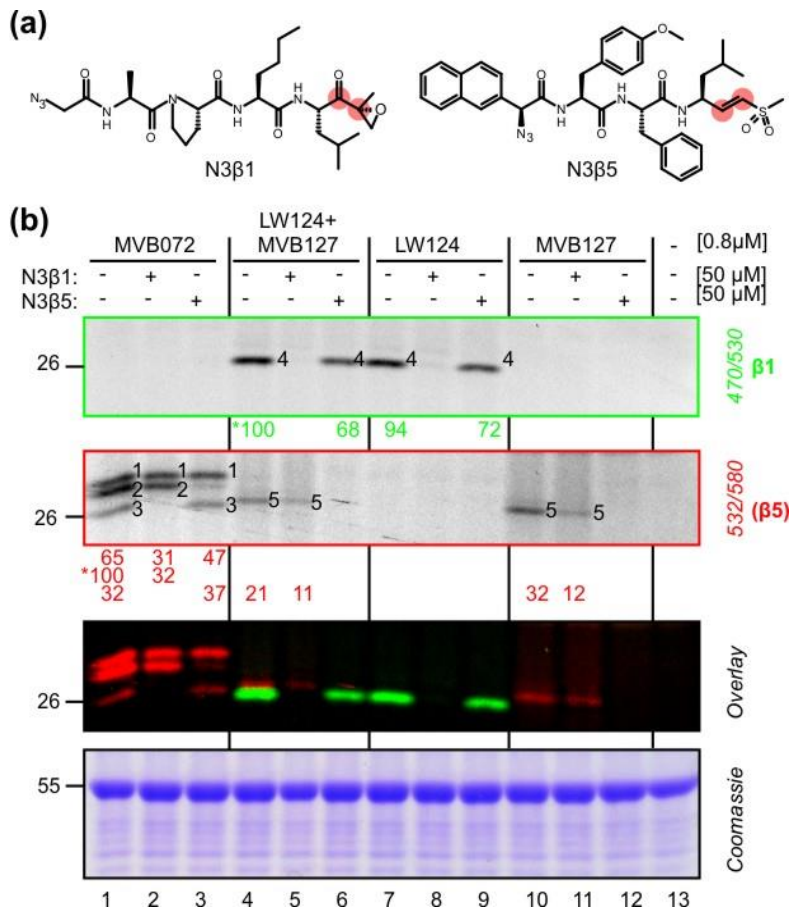
687 **Yang, P., Fu, H., Walker, J.M., Papa, C.M., Smalle, J.A., Ju, Y.M. and Vierstra, R.D.** (2004)
688 Purification of the Arabidopsis 26S proteasome: biochemical and molecular analyses revealed the
689 presence of multiple isoforms. *J. Biol. Chem.* **279**, 6401-6413.

690



691
 692 **Figure 1.** Subunit-specific labeling of Arabidopsis proteasome catalytic subunits
 693 (a) Structures of probes used in this study. MVB072 carries an epoxyketone reactive group, a Ile-Ile-
 694 Ser-Leu tetrapeptide mimic and both a Bodipy TAMRA fluorophore (ex532/em580, red) and a biotin
 695 affinity handle. LW124 contains an epoxyketone reactive group on a Ala-Pro-Nle-Leu tetrapeptide
 696 mimic, and a Bodipy Cy2 fluorophore (ex470/em530, green). MVB127 carries a vinyl sulfone (VS)
 697 reactive group, a MeTyr-Phe-Ile tripeptide and both an azide minitag and a Bodipy TAMRA
 698 fluorophore (ex532/em580, red). RhSylA contains a Michael system reactive group embedded in a
 699 syringolin A (SylA) structure and carries a Rhodamine fluorophore (ex532/em580, red). Sites that are
 700 targeted by the catalytic Thr of the proteasome are highlighted with red circles.
 701 (b) Comparison of the different labeling profiles generated with the four different probes. Arabidopsis
 702 leaf extracts were labeled at pH 7.5 with 0.8 μM MVB072, LW124 and MVB127 for 2 h and with 0.5
 703 μM RhSylA for 30 min. Fluorescent proteins were detected by in-gel fluorescent scanning at two
 704 indicated settings. Numbers on the gel annotate signals caused by the labeled proteins. Numbers below
 705 the gel show the intensity of the fluorescent signals, as a percentage compared to the reference signal
 706 indicated by an asterisk. See **Figure S1** for entire gels. This experiment was performed at least three
 707 independent times with similar results.

708 (c) (Co)labeling of proteasome subunits with the different probes. Arabidopsis leaf extracts were
709 (co)labeled with MVB072, LW124, MVB127 for 2 h. Fluorescent proteins were detected as described
710 in (b). This experiment has been reproduced at least three independent times with similar results.
711



712

713

Figure 2. Subunit-selective inhibitors confirm selective subunit labeling

714

(a) Structures of specific inhibitors for the β1 and β5 proteasome catalytic subunits. N3β1 is an

715

epoxyketone specific inhibitor of the β1 catalytic subunit of the proteasome. N3β5 is a vinyl sulfone

716

based inhibitor that specifically targets the β5 catalytic subunit of the proteasome. Both inhibitors

717

contain an azide group. Reactive groups are indicated with red circles.

718

(b) Subunit-specific inhibitors confirm subunit-selective labeling by LW124 and MVB127.

719

Arabidopsis leaf extracts were pre-incubated with 50 μM N3β1 or N3β5 for 30 min, followed by

720

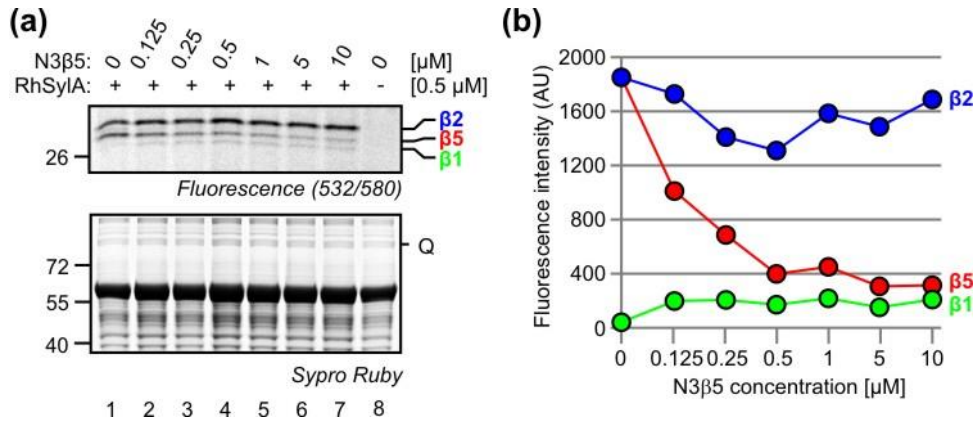
(co)labeling with MVB072, LW124 and MVB127 for 2 h. Fluorescent proteins were detected and

721

annotated with numbers as described in **Figure 1b**. The experiment has been reproduced at least three

722

independent times with similar results.



723

724

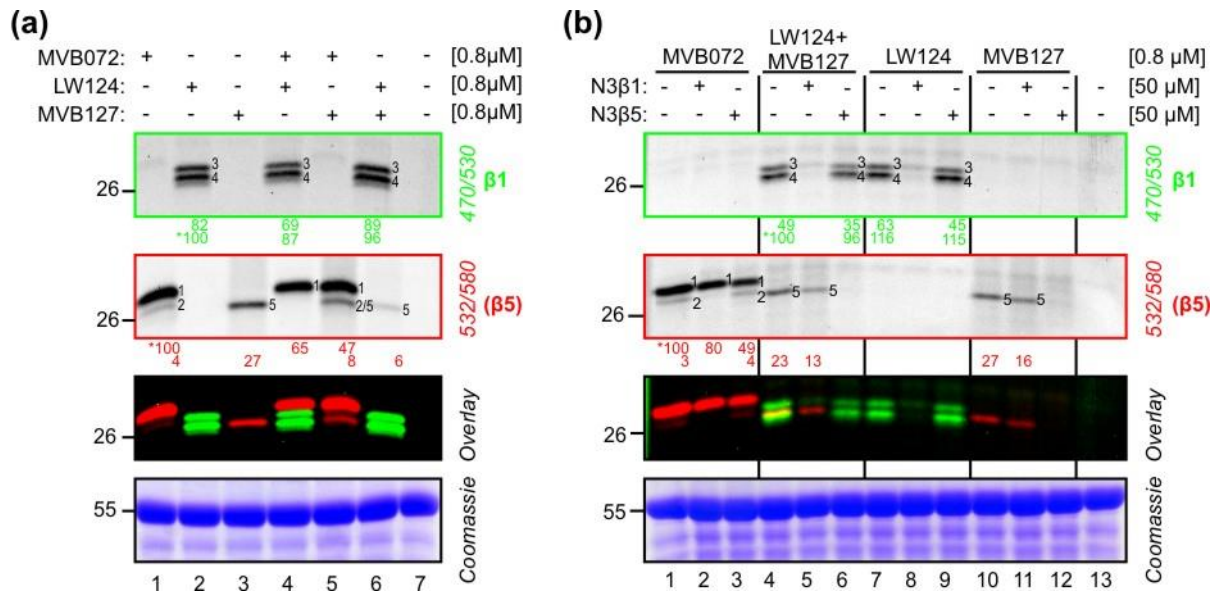
Figure 3. Selective $\beta 2$ labeling using [RhSylA + N3 $\beta 5$]

725

(a) In the presence of N3 $\beta 5$, RhSylA labels $\beta 2$ selectively. Arabidopsis leaf extracts were pre-
 726 incubated with increasing concentrations of the $\beta 5$ selective inhibitor N3 $\beta 5$ for 15 min followed by
 727 labeling with $0.5 \mu\text{M}$ RhSylA for 30 min. Proteins were detected by in-gel fluorescent scanning and
 728 Sypro Ruby staining. This experiment has been repeated four independent times with similar results.

729

(b) Quantification of fluorescence labeling. Fluorescent signals corresponding to the catalytic subunits
 730 $\beta 1$, $\beta 2$ and $\beta 5$ were quantified from fluorescent gels. Fluorescence intensity values were normalized
 731 for loading using the Sypro Ruby signal Q, indicated in (a). Values for the catalytic subunits were
 732 plotted against different N3 $\beta 5$ concentrations. A reproduction of this experiment is shown as Figure
 733 S3.



734

735

Figure 4. Labeling of *N. benthamiana* proteasome with subunit-specific probes

736

(a) Labeling profiling of proteasome specific probes. *N. benthamiana* leaves extracts were (co)labeled at pH 7.5 with 0.8 μM MVB072, LW124 and MVB127 for 2 h. Fluorescent proteins were detected as described in **Figure 1b**. Numbers on gels annotate the different signals caused by labeled proteasome subunits. This experiment has been reproduced at least three independent times with similar results.

737

738

739

740

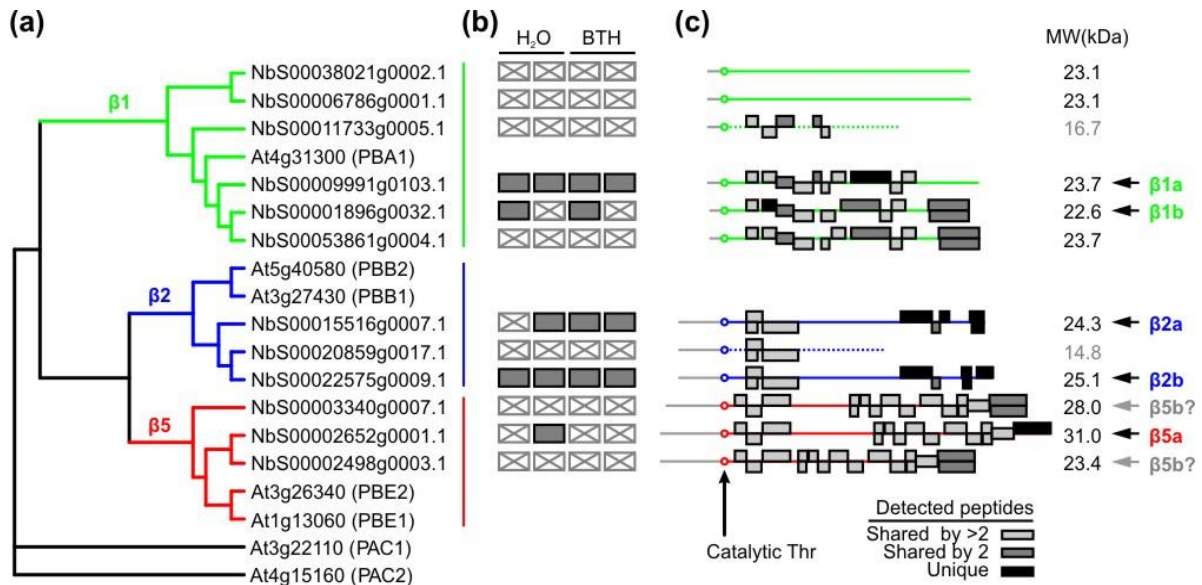
(b) Selective (co)labeling of β1 and β5 of *N. benthamiana*. *N. benthamiana* extracts were pre-incubated with 50 μM of the selective proteasome inhibitors N3β1 and N3β5 for 30 min followed by 2 h (co)labeling with 0.8 μM MVB072, LW124 and MVB127. Fluorescent proteins were detected as described in **Figure 1b**. Shown is a representative gel of three independent biological replicates.

741

742

743

744



745

746

Figure 5. Detection of the expanded proteasome subunit repertoire of *N. benthamiana*

747

(a) Neighbour-joining phylogenetic tree of $\beta 1$, $\beta 2$, and $\beta 5$ catalytic subunits of the proteasome of Arabidopsis and *N. benthamiana*, rooted with the $\alpha 3$ subunit (PAC1 and PAC2).

749

(b) Identification of unique peptides upon MVB072 pull down from *N. benthamiana* leaf extracts.

750

Leaf extracts from plants treated with water or BTH were labeled with MVB072 and the labeled

751

proteins purified on avidin beads, eluted and separated on protein gels. Proteins were digested in-gel

752

with trypsin and the eluted peptides were analyzed twice by mass spectrometry. Filled grey boxes

753

indicate the detection of unique peptides of the respective proteasome subunit, whereas crossed boxes

754

indicate no unique peptides detected.

755

(c) Position of detected peptides of the catalytic subunits. Shown are the peptides that are unique

756

(black); shared with one other subunit (dark grey); or shared with more than one subunit (light grey).

757

Grey lines indicate the propeptide that is removed upon proteasome assembly. The mature protein

758

starts with a catalytic Thr residue. Truncated $\beta 1$ and $\beta 2$ proteasome subunits that may not be

759

functional are shown as dashed lines. The molecular weight (MW) indicates the calculated MW of the

760

mature subunit (without propeptide) in kilo Dalton (kDa). Black arrows indicate subunits that were

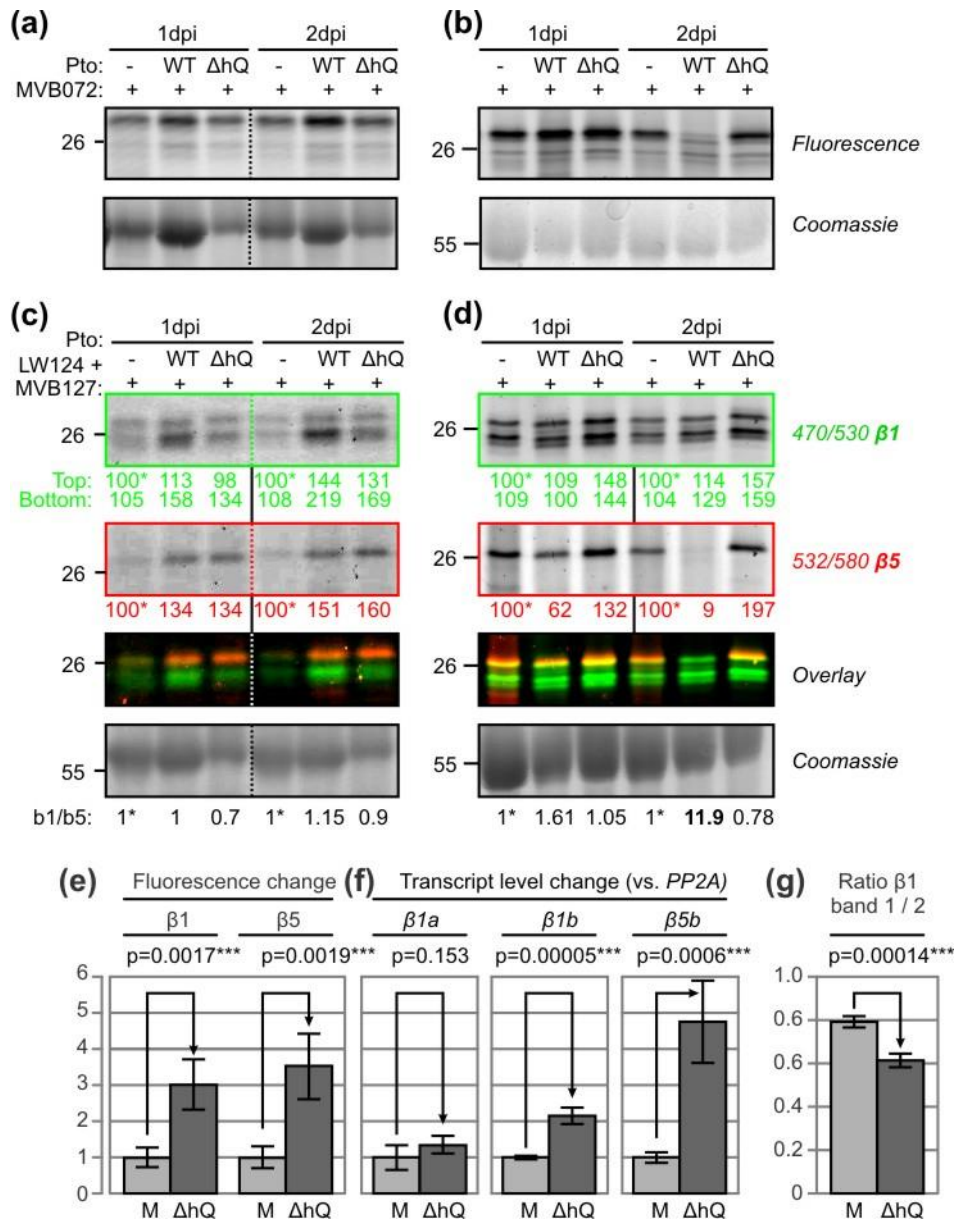
761

identified with unique peptide(s), and the grey arrow indicates the identified $\beta 5$ subunit, in case the

762

truncated $\beta 5$ subunit is considered non-functional.

763



764

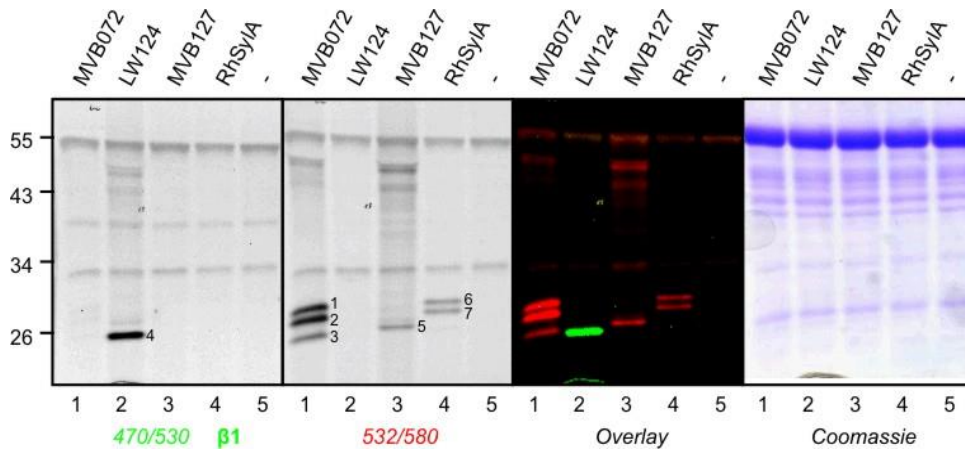
765 **Figure 6.** Uncoupled differential β1 and β5 activities upon bacterial infections.

766 (a-g) *N. benthamiana* leaves were infiltrated with buffer or 10⁶ CFU/mL PtoDC3000(WT) or its
 767 derived *ΔhopQ1-1* mutant PtoDC3000(ΔhQ) and leaf disks were harvested at 1 and 2 dpi. Leaf
 768 extracts were labeled with MVB072 (a,b) or LW124+MVB127 (c,d) and proteins were analyzed as
 769 described in **Figure 1b**. Shown are representatives of independent experiments showing the two
 770 different phenotypes, ranging from induced β1/β5 activities (a,c; Supplemental **Figures S4-S5**), to
 771 suppressed β5 activities (b,d; Supplemental **Figures S6-S8**). (e) Quantified fluorescence for β1
 772 (LW124) and β5 (MVB127) in one experiment with four individuals (n=4 replicates). This experiment
 773 was reproduced twice with similar results (Supplemental **Figures S9**). (f) Relative transcript levels of
 774 *β1a*, *β1b* and *β5b* relative to *PP2A* for the same experiment (n=4 individual plants) as shown in (e). (g)
 775 Relative ratio of the two LW124 signals in the same experiment (n=4 replicates) as shown in (e). This
 776 experiment was reproduced twice with similar results (Supplemental **Figure S9**).

777

778

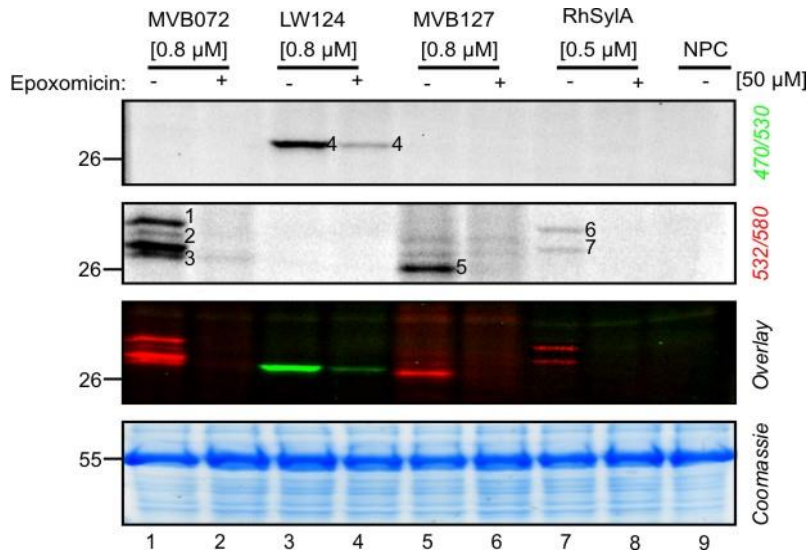
779 **SUPPLEMENTAL FIGURES**



780
781 **Figure S1.** Entire gel showing selective labeling by different proteasome probes.

782 See legend of **Figure 1b** for more information

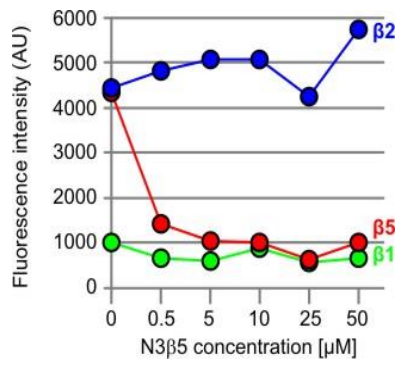
783



784
785 **Figure S2.** Labeling is blocked by pre-incubation with epoxomicin.

786 Arabidopsis leaf extracts were pre-incubated with 50 μ M epoxomicin for 30 min and labeled with
787 MVB072, LW124, MVB127 and RhSylA. Fluorescent proteins were detected at two indicated settings
788 of the fluorescence scanner. Numbers on gels annotate different signals caused by labeled proteasome
789 subunits.

790



791

792 **Figure S3.** Selective $\beta 2$ labeling using [RhSylA + N3 $\beta 5$]

793 Arabidopsis leaf extracts were pre-incubated with increasing concentrations of the $\beta 5$ selective
 794 inhibitor N3 $\beta 5$ for 15 min followed by labeling with 0.5 μM RhSylA for 30 min. Proteins were
 795 detected by in-gel fluorescent scanning and Sypro Ruby staining. Fluorescent signals corresponding to
 796 the catalytic subunits $\beta 1$, $\beta 2$ and $\beta 5$ were quantified from fluorescent gels. Fluorescence intensity
 797 values were normalized for loading using the Sypro Ruby signal. Values for the catalytic subunits
 798 were plotted against different N3 $\beta 5$ concentrations.

799 **Beta 1**

800

801 >MER412180 - Nbs00038021g0002.1

802 MCIFISDSDESHQSN TTTIVGVTYDDGVILGSDIITQLTANVFLCHCALGAYTQVLLLEDARNFLDQETTAAVAEIVGMLLSAYDINNKNM

803 LRTGVLLGGWDKNGGGKIYEIGFSGVMKSNFVGGYGTVDLNDFLEKEWKKMTEEEAEQLVVKALS LNNINSGCGVQTASVNSKEFTTAFH

804 PYATLPKAEKLESEHMNEKPMLECI RAHLLLLLLNINEGL

805

806 >MER411609 - Nbs00006786g0001.1

807 MCIFIIDSEKSHQSN TTTIVGVTYDDGVMLGSDIITKLTASVFLCHCALGADTQVLLLEDARNFLDQETTATVAEIVGMVLSAYDINNKNM

808 LRTGVLLGGWDKNGGGKIYEIGFSGVMKSNFVGGYGAVDLNDFLEKEWKKGLTEEEAEQLVVKALS LNNINSGCGAQTASVNSKGFTTDF

809 HPYVILPKAEKLELENMNEKPMLECI RAHLLLLLLNIDEGL

810

811 >MER412281 - Nbs00011733g0005.1 coverage after T:

812 MDKSLLDVEQAHSMTIIGVTYNRGVVLGANSRTSTGMYVANRASDKITQLTDNVYVCRSGSAADSQVVSVDYVRYFLHQHMIQLGQPATVKVA

813 ANLVRLLSYNNKAMLQTMIVGGWDKYEYGVKYMGLLGAHSWNSLLLLLEVCCQSVLFEYLILLPRSTLLVN

814

815 >MER412197 - Nbs00009991g0103.1 - β 1a coverage after T:

816 MDKSLLDVEQPHSMGTIIGVTYNGGVVLGADSRSTSTGMYVANRASDKITQLTDNVYVCRSGSAADSQVVSVDYVRYFLHQHTIQLGQPATVKVA

817 ANLVRLLSYNNKAMLQTMIGGWDKYEGGKIYGVPLGGTLLLEQPF AIGGSGSSYLYGFFDQAWREGMTQEEAEKLVVTAVSLAIARDGASGGV

818 VRTVTINKDGVTRKFPYGD TPLWHEEIEAVNSLLDIVPAASPEPMVS

819

820 >MER411801 - Nbs00001896g0032.1 - β 1b coverage after T:

821 MENTDQVDPHSMGTIIGVTYNGGVVLGADSRSTSTGMYVANRASDKITQLTDNVYVCRSGSAADSQIVSDYVRYFLHQHTIQLGQPATVKVAAN

822 LTRLQTMIGGWDKYEGGKIYGIPLGGTVLEQPF AIGGSGSSYLYGFFDQAWKEGMTQEEAEKLVVTAVSLAIARDGASGGVVRTVTINKDGA

823 TRKFPYGD SLQWHEEIEPVNSLLDVVSASSPDPMVS

824

825 >MER411773 - Nbs00053861g0004.1 coverage after T:

826 MENTDQVDPHSMGTIIGVTYNGGVVLGADSRSTSTGMYVANRASDKITQLTDNVYVCRSGSAADSQIVSDYVRYFLHQHTIQLGQPATVKVAAN

827 LTRLQTMIGGWDKYEGGKIYGIPLGGTVLEQPF AIGGSGSSYLYGFFDQAWKEGMTQEEAEKLVVTAVSLAIARDGASGGVVRTVTINKDGA

828 TRKFPYGD SLQWHEEIEPVNSLLDVVSASSPDPMVS

829

830 **Beta 2**

831

832 >MER411637 - Nbs00015516g0007.1 - β 2a coverage after T:

833 MASKAATDVPKGGGFSFDLCRRNEMLVNKLGRSPFLKTGTIVGLIFQDGVILGADTRATEGPIVADKNCEKIHMAPNIYCCGAGTAADTEA

834 VTDMVSSQLKLRHRYHTGRESRVVTALTLKTHLFSYQGYVSAALVGGVDVTGPHLHTIYPHGSTD TLPYATMGGSLAAMAIFESKYREGLSK

835 DEGIKLVAEAILSGVFNDLGSNSVDICITRGNTEYLRNHMLPNPRTYPQKEVLLTKITPLRERFEVIEGGDAMEE

836

837 >MER411855 - Nbs00020859g0017.1

838 MTAKATMDVPKGGGFSFDLCRRNEMLVNKLGRSPFLKTGTIVGLIFQDGVILGADTRATEGPIVADKNCEKIHMAPNIYCCGAGTAADTEA

839 VTDMVSSQLKLRHRYHTGRESRVVTALTLKSHLFSYQGHVSAALVGGVDVTGPHLHTIYPHGSTD TLPYATNGLWFPNSNGYL

840

841 >MER411772 - Nbs00022575g0009.1 - β 2b coverage after T:

842 MTAKATMDVPKGGGFSFDLCRRNEMLVNKLGRSPFLKTGTIVGLIFQDGVILGADTRATEGPIVADKNCEKIHMAPNIYCCGAGTAADTEA

843 VTDMVSSQLKLRHRYHTGRESRVVTALTLKSHLFSYQGHVSAALVGGVDVTGPHLHTIYPHGSTD TLPYATMGGSLAAMAIFESKYREGMNR

844 DEGIKLVAEAILSGVFNDLGSNSVDICITRGNTEYLRNHLSNPRTYPQKGYSPFKKTEVLLTKITPLREIVQVIEGGDAMEE

845

846

847 **Beta 5**

848

849 >MER412029 - Nbs00003340g0007.1 - β 5b coverage after T:

850 MMKIDFSGLEPTAPLKGESSVLCDGILSSPSFQIPNTNKEAIQMVKPAKTTLAFIFKGGVMVAADSRASMGYISSQSVKIIIEINPYMLG

851 TMAGGAADCQFWHRNLGKKSQTQPKGMSDAKTSDLBGYP LNLGDALCESGKVESTAEPLKRLHELANKRRISVAGASKLLANILYSYRG

852 MGLSVGTMIAGWDEKGPGLYVDSEGGRLKGNRFSVSGSPYAYGVLD SGYRFDLSVEEAAELARRAIYHATFRD GASGGVASVYHVGPNGWK

853 LSGDDV GELHYNYPVELESVEQEMAEVPVA

854

855 >MER411662 - Nbs00002652g0001.1 - β 5a coverage after T:

856 MMKIDFSGLEPTAPIKGESSELCDGILSSPSFQIPNATNFDGFQKEAIQMVKPAKTTLAFIFKGGVMVAADSRASMGYISSQSVKIIIEIN

857 PYMLGTMAGGAADCQFWHRNLGKENANFVAIVILIDHGHLYKCKWPILKEDLIAVLEHLYKEGKEKKNMIVRGICAGWILLVVELCVVCRLLH

858 ELANKRRISVAGASKLLANILYSYRGMGLSVGTMIAGWDEKGPGLYVDSEGGRLKGNRFSVSGSPYAYGVLD SGYRFDLSVEEAAELARRAI

859 YHATFRD GASGGVASVYHVGPNGWKLSGDDV GELHYSYYPVELESVEQEMAEVPVA

860

861 >MER412196 - Nbs00002498g0003.1 coverage after T:

862 MMKIDFSGLEPTAPIKGESSELCDGILSSPSFQIPNATNFDGFQKEAIQMVKPAKTTLAFIFKGGVMVAADSRASMGYISSQSVKIIIEIN

863 PYMLGTMAGGAADCQFWHRNLGKKSQTQPKGMSDAKTSDLBGYP LNLGDALCESGKVESTAEPLKRLHELANKRRISVAGASKLLANILYSYRGMGLSVGTMIAGWDEKGPGLYVDSEGGRLKGNRFSVSGS

864 PYAYGVLD SGYRFDLSVEEAAELARRAIYHATFRD GASGGVASVYHVGPNGWKLSGDDV GELHYNYPVELESVEQEMAEVPVA

865

866

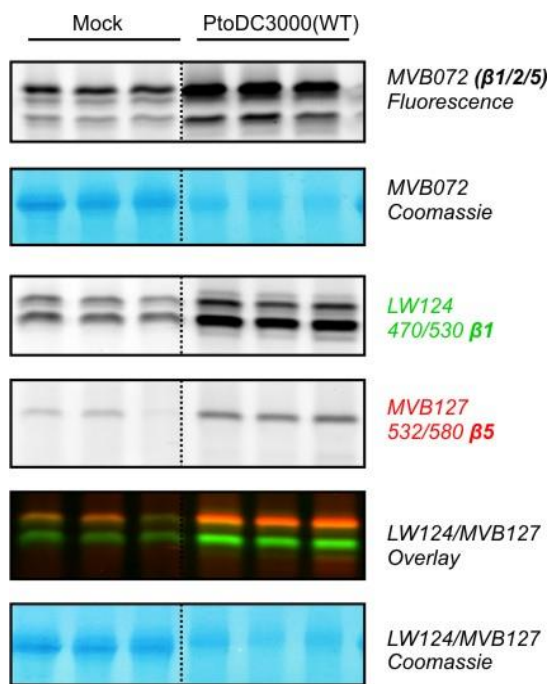
867 **Figure S3.** Identified peptides mapped on the protein sequences of the catalytic subunits of

868 the *N. benthamiana* proteasome. Shown are the catalytic Thr (blue); unique peptides (red);

869 peptides shared by two proteins (dark grey); peptides shared by more than two proteins (light grey);

870 peptides that overlap with a larger peptide (missed cleavage, underlined). Subunits that are too short

871 are printed with grey letters.

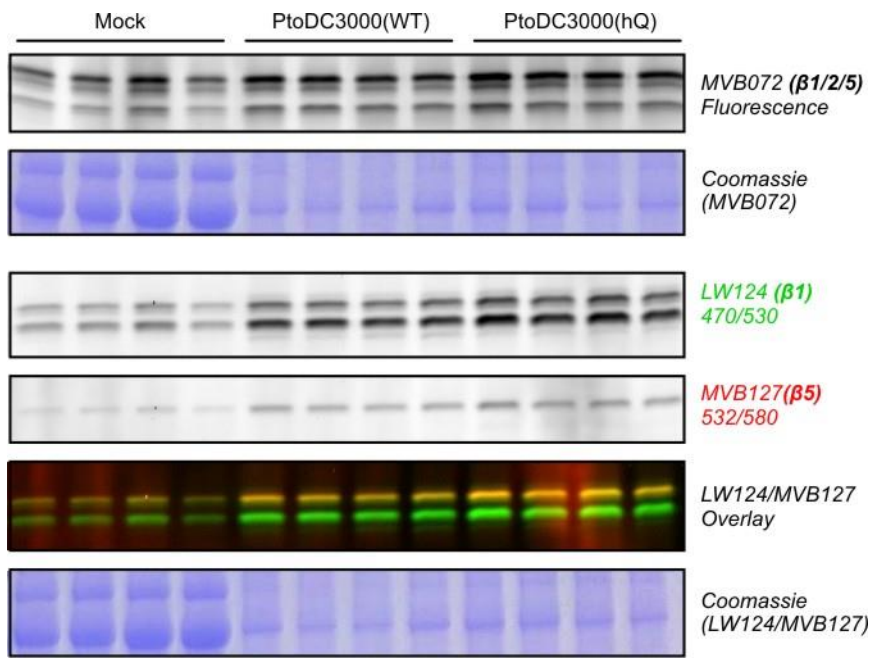


872

873 **Figure S4.** Increased proteasome activity upon WT infection. Shown is one experiment

874 containing three biological replicates.

875

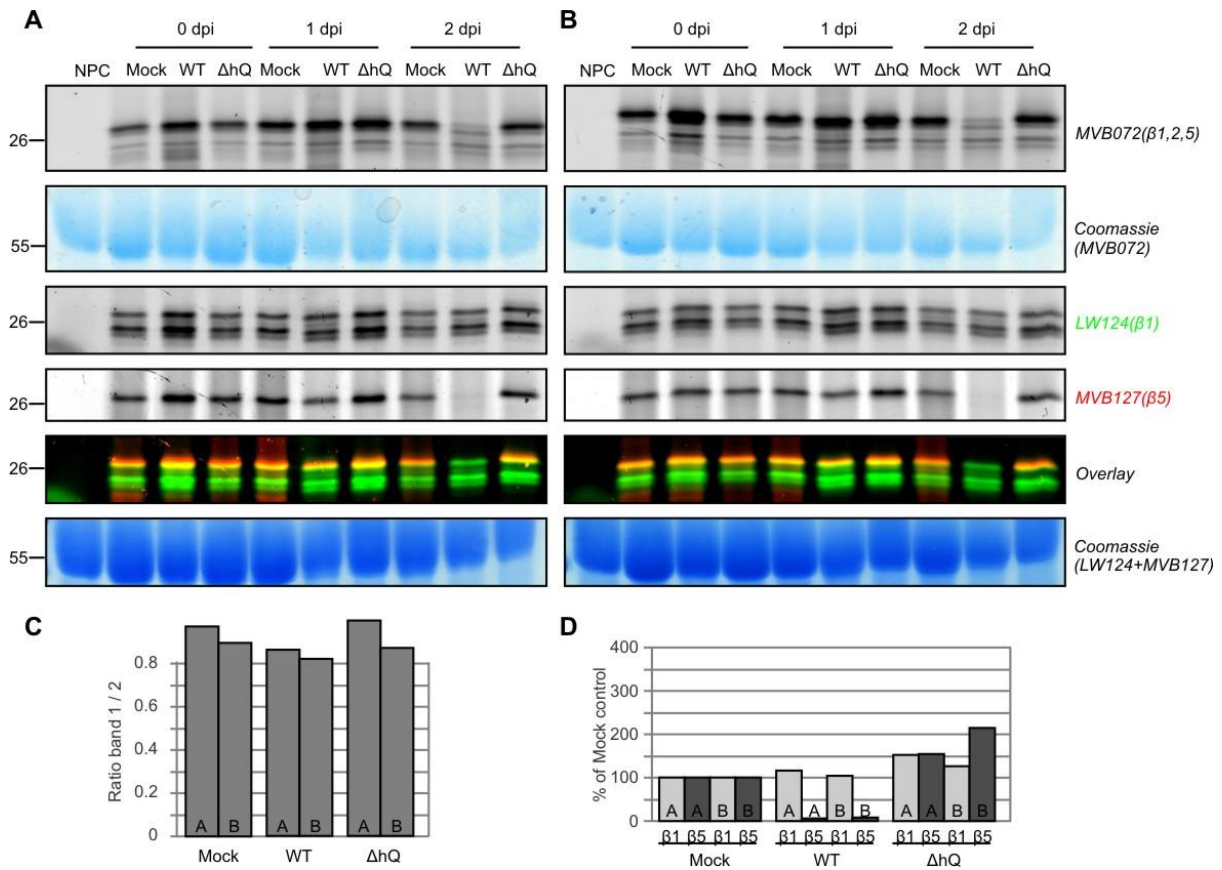


876

877 **Figure S5.** Increased proteasome activity upon WT infection. Shown is one experiment

878 containing four biological replicates. See **Figure 6** for more details.

879



880

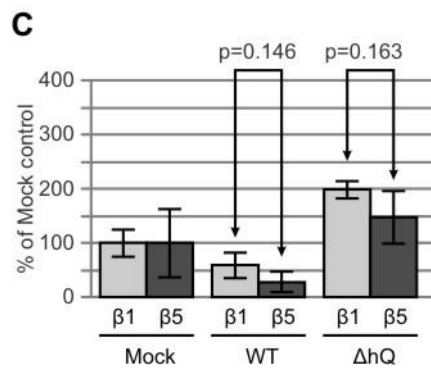
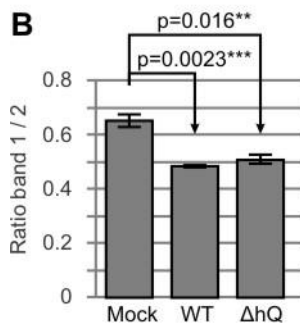
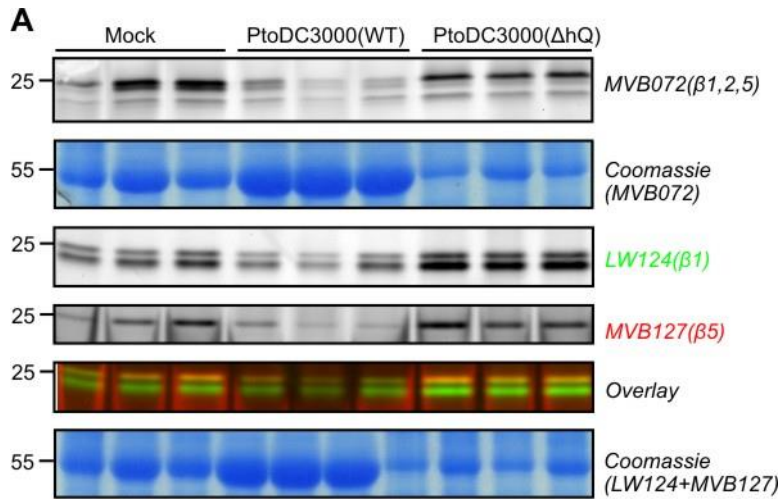
881

882

883

884

Figure S6. Suppressed β5 labeling upon WT infection. **A, B**) Shown is one experiment containing two biological replicates. Part of the right half of this figure is shown in **Figure 6bd**. **C**) Ratio of the two β1 signals. **D**) Fluorescent intensity of the signals, normalized to the Mock control. See Figure 6 for more details.



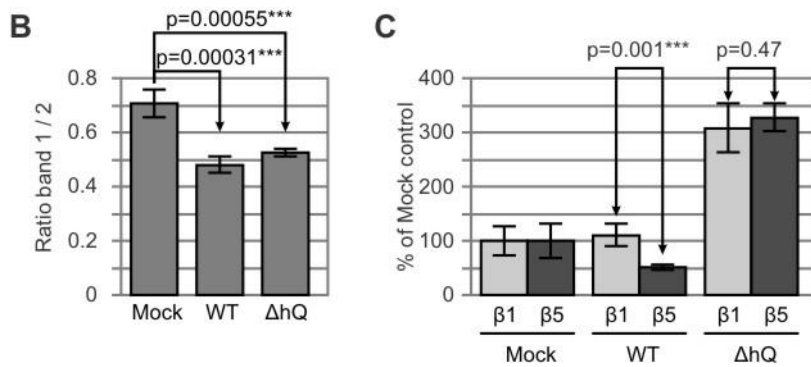
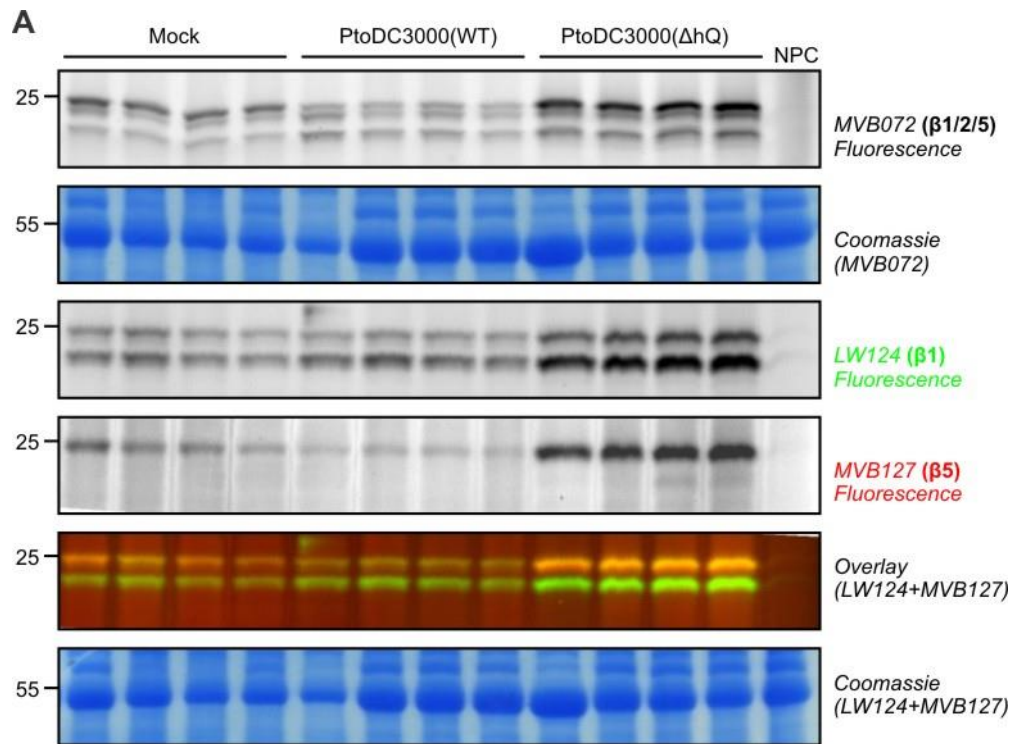
885

886

887

888

Figure S7. Suppressed β5 labeling upon WT infection. Shown is one experiment containing three biological replicates. **B)** Ratio of the two β1 signals. **C)** Fluorescent intensity of the signals, normalized to the Mock control. See Figure 6 for more details.

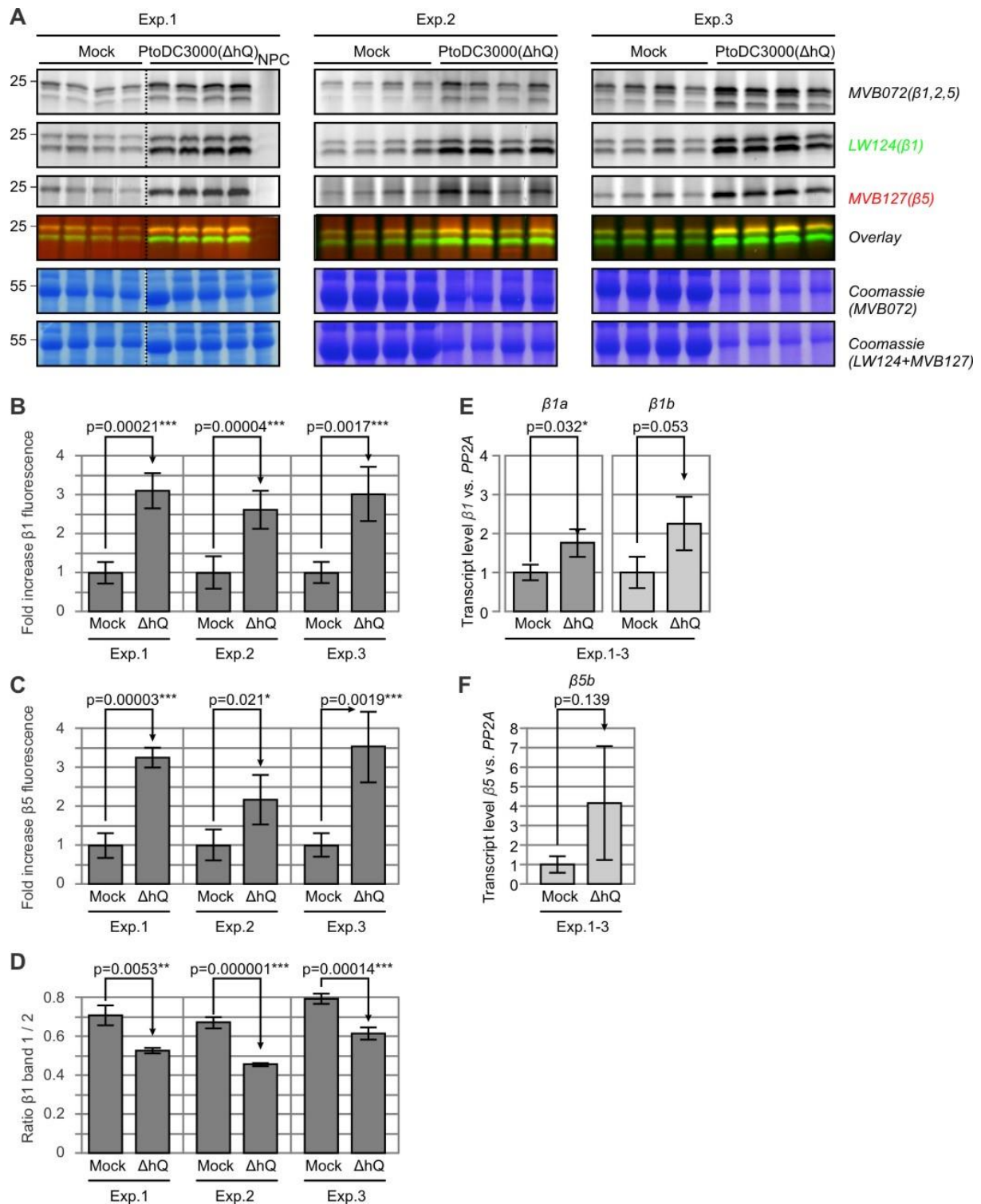


889

890 **Figure S8.** Suppressed β5 labeling upon WT infection. Shown is one experiment containing four

891 biological replicates. **B)** Ratio of the two β1 signals. **C)** Fluorescent intensity of the signals,

892 normalized to the Mock control. See Figure 6 for more details.



893

894

895

896

897

898

899

900

Figure S9 Altered proteasome activity upon infection with PtoDC3000(ΔhQ). **A**) Shown are three independent experiments, each containing four biological replicates. **B, C**) Fluorescence intensity normalized to the Mock control for each of the three experiments. **D**) Ratio of β1 signals 1 and 2 for each of the three experiments. **E, F**) qRT-PCR, performed on the three biological experiments. Replicates of each biological experiment were mixed (n=4) and the average of expression and standard deviation were calculated for the three biological experiments. See **Figure 6** for more details.

901 **Table S1:** Identified peptides of catalytic subunits*.

Peptide sequence	u/s	score	protein	BTH		H2O	
				MS1	MS2	MS1	MS1
EGMTQEAEAK	s	175.5	beta 1	2	2	2	2
FYPGDSLQLWHEELEPVNSLLDVVSASSPDPMVS	s	110.2	beta 1	1	0	2	0
ITQLTDNVVYVCR	s	283.5	beta 1	4	3	4	4
IYGIPLGGTVLEQPPFAIGGSGSSYLYGFFDQAWK	s	155.5	beta 1	2	1	2	1
KFYPGDSLQLWHEELEPVNSLLDVVSASSPDPMVS	s	57.14	beta 1	1	0	2	0
LLSYNNK	s	128.5	beta 1	1	1	1	1
LQTGMIIGGWDK	s	151.7	beta 1	3	2	3	3
LVVTAVSLAIAR	s	168.0	beta 1	3	2	2	2
SGSAADSQIVSDYVR	s	254.9	beta 1	2	3	3	1
SGSAADSQVVS DYVR	s	299.2	beta 1	2	2	2	2
TSTGMVYVANR	s	228.2	beta 1	5	5	6	5
VAANLVR	s	137.8	beta 1	1	1	1	1
YFLHQHTIQLGQPATVK	s	298.1	beta 1	3	4	4	3
ATEGPIVADK	s	199.3	beta 2	2	3	2	2
ATEGPIVADKNCEK	s	177.0	beta 2	0	0	1	0
GNTEYLR	s	129.7	beta 2	1	1	1	1
IHYMAPNIYCCGAGTAADTEAVTDMVSSQLK	s	138.4	beta 2	1	0	3	0
IIEINPYMLGTMAGGAADCQFWHR	s	103.6	beta 2	2	1	3	0
AIYHATFR	s	204.8	beta 5	1	0	1	0
ASMGYISSQSVK	s	214.6	beta 5	6	4	4	5
DGASGGVASVYHVGPNGWK	s	287.0	beta 5	4	2	4	2
FDLSVEEAAELAR	s	373.7	beta 5	3	4	2	3
FSVSGSPYAYGVLD SGYR	s	242.7	beta 5	4	5	6	5
GGVMVAADSR	s	123.0	beta 5	3	3	3	5
GMGLSVGTMIAGWDEK	s	214.9	beta 5	7	4	8	6
GPGLYYV DSEGGR	s	136.9	beta 5	1	1	2	2
ISVAGASK	s	124.1	beta 5	0	0	1	0
KLSGDDV GELHYNYYPVELESVEQEMAEVPVA	s	57.9	beta 5	2	0	2	0
LHELANK	s	141.0	beta 5	2	1	1	1
LHELANKR	s	141.5	beta 5	1	1	1	0
LLANILYSYR	s	190.6	beta 5	1	1	1	2
LSGDDV GELHYNYYPVELESVEQEMAEVPVA	s	68.84	beta 5	2	2	4	2
RAIYHATFR	s	128.5	beta 5	1	0	1	0
RISVAGASK	s	120.6	beta 5	0	0	1	0
ITQLDNDNVVYVCR	u	218.0	Nbs00001896g0032.1	1	1	2	1
KLSGDDV GELHYSYYPVELESVEQEMAEVPVA	u	50.03	Nbs00002652g0001.1	0	0	1	0
IYGVPLGGTLLEQPPFAIGGSGSSYLYGFFDQAWR	u	111.2	Nbs00009991g0103.1	0	1	0	1
ERVEIEGGDAMEE	u	197.1	Nbs00015516g0007.1	1	0	1	0
NHMLPNPR	u	94.16	Nbs00015516g0007.1	1	0	1	0
LVAEAILSGVFNDLGSGSNVDICITK	u	112.5	Nbs00015516g0007.1	1	1	0	0
VEVIEGGDAMEE	u	202.0	Nbs00015516g0007.1	1	0	1	0
KTEVLLTK	u	181.5	Nbs00022575g0009.1	2	1	2	1
EIVQVIEGGDAMEE	u	227.6	Nbs00022575g0009.1	5	1	4	1
LVAEAILSGVFNDLGSGSNVDICVITK	u	119.2	Nbs00022575g0009.1	1	1	1	0
TEVLLTK	u	143.6	Nbs00022575g0009.1	2	1	2	1

902 *, unique (u) or shared (s); highest peptide score; protein hit; spectral counts in the two pull down
903 experiments, each analyzed twice by MS.